

Probing neutrino interactions and dark radiation with gravitational waves

Marilena Loverde and Zachary J. Weiner

Department of Physics, University of Washington,
Seattle, WA 98195, U.S.A.

E-mail: mloverde@uw.edu, zweiner@uw.edu

Abstract. After their generation, cosmological backgrounds of gravitational waves propagate nearly freely but for the expansion of the Universe and the anisotropic stress of free-streaming particles. Primordial signals—both that from inflation and the infrared spectrum associated to subhorizon production mechanisms—would carry clean information about the cosmological history of these effects. We study the modulation of the standard damping of gravitational waves by free-streaming radiation due to the decoupling (or recoupling) of interactions. We focus on nonstandard neutrino interactions in effect after the decoupling of weak interactions as well as more general scenarios in the early Universe involving other light relics. We develop semianalytic results in fully free-streaming scenarios to provide intuition for numerical results that incorporate interaction rates with a variety of temperature dependencies. Finally, we compute the imprint of neutrino interactions on the B -mode polarization of the cosmic microwave background, and we comment on other means to infer the presence of such effects at higher frequencies.

Contents

1	Introduction	1
2	Gravitational waves and relativistic particles	2
2.1	Cosmological perturbation theory	3
2.2	Modeling interacting radiation	6
2.3	Integral solutions	8
3	Damping of inflationary gravitational waves	10
3.1	Results in noninteracting scenarios	10
3.2	Results in interacting scenarios	12
4	Damping of causal gravitational waves	15
4.1	Results in noninteracting scenarios	15
4.2	Results in interacting scenarios	17
5	Discussion	19
A	Numerical implementation	21
B	Semianalytic results for inflationary gravitational waves	22

1 Introduction

Observing a background of low-frequency gravitational waves remains a top science goal for contemporary and upcoming cosmic microwave background (CMB) experiments [1–11]. A detection of primordial gravitational waves, on top of the confirmed predictions that the initial conditions of large-scale density fluctuations would be adiabatic, nearly Gaussian, and nearly scale invariant [12, 13], would all but confirm an early phase of quasi de Sitter expansion as the origin of structure in the Universe [14–21]. In the simplest models of inflation, the amplitude of the gravitational wave spectrum directly measures the (otherwise unknown) energy scale of the fundamental physics at play. The latest constraints limit the amplitude of such tensor fluctuations to be smaller than 0.036 times its scalar counterpart at the 95% confidence level [10], corresponding to an upper energy scale of 1.4×10^{16} GeV. If the energy scale of inflation is not dramatically smaller than this current limit, then upcoming experiments could observe the signature of primordial gravitational waves in the *B*-mode (curl-like) polarization of the CMB anisotropies.

At the same time, interferometric experiments and pulsar timing arrays have opened a new window on relativistic astrophysical phenomena—principally via gravitational wave signals from mergers of compact objects or black holes [22–24]. For the cosmologist, aside from the potential to probe phase transitions [25–30], topological defects [31–37], particle production [38–42], and primordial black holes [43–48], direct detection experiments offer a high-frequency anchor which could provide complementary information about the possible primordial background from inflation [49–60]. By constraining gravitational waves over a large range in frequency (at scales far smaller than those that would imprint upon the observable CMB), gravitational wave experiments could provide a unique view into the physics of the very early Universe (see Refs. [9, 61, 62] for reviews).

Measurements of inflationary gravitational waves would inform more physics than just that of inflation itself. The present-day spectrum is sensitive to the thermal history of the Standard Model plasma and the expansion history of the Universe—especially to large departures from radiation domination [63–69]. Moreover, cosmological gravitational waves also interact with relativistic particles. Once the weak interactions become inefficient (when the Universe was about a second old), Standard Model neutrinos begin free streaming, reducing the amplitude of inflationary gravitational waves by

about 20% on scales larger than the horizon at that time [70]. In general, gravitational waves probe the interaction history of the entire relativistic content of the Universe. In this paper we investigate the imprints of beyond-the-Standard-Model interactions of neutrinos (or other hypothetical particles) on the stochastic gravitational wave background.

Within the Standard Model (SM), neutrinos are neutral and couple only via the weak interactions, and many of their properties are largely inaccessible to current laboratory experiments. Yet for much of the Universe’s history neutrinos were the second-most abundant species, for which reason cosmological observations provide substantial information about their dynamics. After the weak interactions become inefficient, the cosmological role of neutrinos is purely gravitational. At least two of the neutrinos are massive, and cosmological data place upper limits on their absolute mass scale via their contribution to the expansion rate and growth of structure when nonrelativistic [71, 72]. At earlier times when they are relativistic, the observable signatures of spatial perturbations to the neutrino distribution is predominantly governed by whether they scatter frequently (and so are fluidlike) or interact rarely (and instead free stream) [73]. In the latter case, their anisotropic stress not only impacts baryon acoustic oscillations [73–76] but is also responsible for the aforementioned damping of gravitational waves. Measurements of the temperature anisotropies of the CMB confirm that most (if not all) of the energy density in neutrinos is free-streaming [75, 77–79]; however, it remains possible that neutrinos have self-interactions that decouple at some time around recombination [79–87].

Relativistic particles interact not only with the superhorizon gravitational waves frozen out during inflation but also with the low-frequency tail of stochastic backgrounds generated by subhorizon processes [88, 89]. A promising candidate is that from the electroweak phase transition, which could be detected by LISA if the transition is first order [30]. Free-streaming, relativistic particles would leave a characteristic signature on the infrared, “causal” part of the spectrum, altering its power-law dependence or even inducing oscillatory features. The dynamics of causal gravitational waves are largely agnostic to the details of the underlying source, effectively reducing to a transfer function encoding propagation effects to the present day, similar to that applicable to inflationary gravitational waves. We also investigate the imprints of self-interacting radiation in this complementary scenario.

In the remainder of this paper, we first present the theory of cosmological perturbations in application to relativistic degrees of freedom and gravitational waves (in Section 2). In Section 3 we develop semianalytic solutions for the effect of noninteracting neutrinos on primordial gravitational waves from inflation, building intuition with which to understand numerical results for interacting neutrinos. We then consider “causal” gravitational wave backgrounds from subhorizon sources in Section 4. These two scenarios are mathematically distinguished by the gravitational waves’ initial conditions—a frozen-out amplitude or a sudden jump in velocity, respectively—each exhibiting a starkly different response to free-streaming radiation. Because the anisotropic stress sourced by collisionless radiation decays with expansion inside the horizon, the causal and inflationary scenarios together provide a nearly complete treatment of the effect of free-streaming radiation on gravitational waves. Though we focus on the effect of neutrinos for concreteness, our analysis extends straightforwardly to other, hypothetical dark radiation species.¹ In Section 5 we conclude with a discussion of future prospects for constraining neutrino interactions and hypothetical new degrees of freedom in CMB B -modes and direct gravitational wave measurements. Appendix A details our numerical implementation, and Appendix B outlines a semianalytic calculation of the damping effect employed in Section 3.

2 Gravitational waves and relativistic particles

We first review the well-established theory of the dynamics of gravitational and matter perturbations in the early Universe in application to the coupling of gravitational waves and relativistic species (of any spin). Gravitational waves also interact with other types of matter, including relativistic axions [90, 91], nonrelativistic and collisional matter [92–95], and vector fields [96–99]; some of these scenarios are not captured by the kinetic theory treatment we review. We neglect any chemical potential that would be requisite to describe, e.g., chiral fermions and polarized gravitational waves [100–103].

¹The rest mass of neutrinos or other dark radiation is irrelevant so long the particles are relativistic while the scales of interest enter the horizon.

2.1 Cosmological perturbation theory

Since we are interested only in gravitational wave observables, we consider a Friedmann-Lemaître-Robertson-Walker (FLRW) spacetime perturbed only by a tensor mode h_{ij} :

$$ds^2 = a(\tau)^2 (-d\tau^2 + [\delta_{ij} + h_{ij}(\tau, \mathbf{x})] dx^i dx^j). \quad (2.1)$$

Primes indicate derivatives with respect to the conformal time τ , and we denote the conformal Hubble parameter as $\mathcal{H}(\tau) \equiv a'(\tau)/a(\tau)$, in terms of which the (standard) Hubble parameter is $H(\tau) = \mathcal{H}(\tau)/a(\tau)$. Repeated spatial (Latin) indices are contracted with the Kronecker delta function regardless of their placement. The tensor perturbation h_{ij} is transverse ($\partial_i h_{ij} = 0$) and traceless ($h_{ii} = 0$); its Fourier modes may therefore be expanded in terms of two polarizations λ as

$$h_{ij}(\tau, \mathbf{x}) = \int \frac{d^3k}{(2\pi)^3} h_{ij}(\tau, \mathbf{k}) e^{i\mathbf{k}\cdot\mathbf{x}} \equiv \int \frac{d^3k}{(2\pi)^3} e^{i\mathbf{k}\cdot\mathbf{x}} \sum_{\lambda} h_{\lambda}(\tau, \mathbf{k}) \epsilon_{ij}^{\lambda}(\mathbf{k}). \quad (2.2)$$

We do not have cause to pick a particular basis of polarization tensors $\epsilon_{ij}^{\lambda}(\mathbf{k})$, but any choice must likewise be transverse and traceless. The Einstein equation for h_{ij} , decomposed onto this basis, takes the form of two inhomogeneous, damped waved equations,

$$h_{\lambda}'' + 2\mathcal{H}h_{\lambda}' - \partial_k \partial_k h_{\lambda} = \frac{2a^2}{M_{\text{pl}}^2} \pi_{\lambda}^T. \quad (2.3)$$

Gravitational waves are sourced by the transverse and traceless component π_{ij}^T of the perturbation to the stress tensor, δT_j^i .

Gravitational waves carry an effective energy density which, deep inside the horizon (i.e., $k \gg \mathcal{H}$), is [104–106]

$$\bar{\rho}_{\text{GW}}(\tau) = \frac{M_{\text{pl}}^2}{8a^2} \langle h'_{ij} h'_{ij} + \partial_k h_{ij} \partial_k h_{ij} \rangle, \quad (2.4)$$

where the angled brackets a spatial average. The observable of interest is the fractional contribution by gravitational waves of a given wavenumber to the background energy density of the Universe, $\bar{\rho}(\tau) = 3H(\tau)^2 M_{\text{pl}}^2$. We therefore define the spectral abundance of gravitational waves,

$$\Omega_{\text{GW}}(\tau, k) = \frac{1}{\bar{\rho}(\tau)} \frac{d\bar{\rho}_{\text{GW}}(\tau)}{d \ln k}. \quad (2.5)$$

Since gravitational waves deep inside the horizon are effectively undamped harmonic oscillators, $|h'_{\lambda}(\tau, \mathbf{k})| \approx |k h_{\lambda}(\tau, \mathbf{k})|$. The effective energy density Eq. (2.4) may then be expressed as an integral over wavenumber by substituting the inverse Fourier transform of h_{ij} , Eq. (2.2). In terms of the dimensionless power spectrum of h_{λ} ,

$$\langle h_{\lambda_1}(\tau, \mathbf{k}_1) h_{\lambda_2}(\tau, \mathbf{k}_2) \rangle \equiv (2\pi)^3 \delta^3(\mathbf{k}_1 + \mathbf{k}_2) \delta_{\lambda_1 \lambda_2} \frac{2\pi^2}{k_1^3} \Delta_{\lambda_1}^2(\tau, k_1), \quad (2.6)$$

we may therefore write the spectral abundance of gravitational waves as

$$\Omega_{\text{GW}}(\tau, k) = \frac{1}{12} \left(\frac{k}{\mathcal{H}(\tau)} \right)^2 \sum_{\lambda} \overline{\Delta_{\lambda}^2(\tau, k)}. \quad (2.7)$$

where the overbar denotes a time average (i.e., over oscillations to ensure the validity of taking $|h'_{\lambda}| \approx |k h_{\lambda}|$). The spectrum evaluated in the early Universe is related to that at the present day (at τ_0) by the transfer function [9, 68]

$$\Omega_{\text{GW}}(\tau_0, k) h^2 = \Omega_{\text{rad}}(\tau_0) h^2 \frac{g_{\star}(\tau)}{g_{\star}(\tau_0)} \left(\frac{g_{\star S}(\tau)}{g_{\star S}(\tau_0)} \right)^{-4/3} \Omega_{\text{GW}}(\tau, k) \quad (2.8)$$

and would be observed at present-day frequencies related to wavenumber k by

$$f = \frac{k/2\pi a(\tau)}{\sqrt{H(\tau)M_{\text{pl}}}} [\Omega_{\text{rad}}(\tau_0)H_0^2 M_{\text{pl}}^2]^{1/4} \left(\frac{g_*(\tau)}{g_*(\tau_0)}\right)^{1/4} \left(\frac{g_{*S}(\tau)}{g_{*S}(\tau_0)}\right)^{-1/3}. \quad (2.9)$$

Here g_* and g_{*S} are the numbers of relativistic degrees of freedom in energy and entropy density, respectively. Note that the present-day abundance of radiation, evaluated as if neutrinos are massless, is $\Omega_{\text{rad}}(\tau_0)h^2 \approx 4.2 \times 10^{-5}$ [13] and that $H_0/h \equiv 100 \text{ km s}^{-1}/\text{Mpc} \approx 3.24 \times 10^{-18} \text{ Hz}$.

Making further progress requires specifying the matter content that contributes to the anisotropic stress tensor π_λ^T . Following the standard prescription [107], we solve the Boltzmann equation for the phase space density of particles, expanded into background and perturbed components as

$$f(\tau, \mathbf{x}, q, \hat{q}) \equiv \bar{f}(\tau, q) [1 + \Psi(\tau, \mathbf{x}, q, \hat{q})]. \quad (2.10)$$

Like Ref. [107], we parameterize the functional dependence of the distribution function in terms of spacetime \mathbf{x} and τ , comoving momentum $q = ap$ (where p is the magnitude of the proper momentum), and propagation direction $\hat{q}_i \equiv q_i/q$. We also define the comoving energy $\mathcal{E} = aE$ in terms of the particle energy $E = \sqrt{p^2 + m^2}$. While we consider only relativistic particles with $p \gg m$, for which $\mathcal{E} = q$, we retain the distinction for the time being. The Boltzmann equation is

$$\frac{d}{d\tau} f(\tau, \mathbf{x}, q, \hat{q}) = \mathcal{C}[f], \quad (2.11)$$

where $\mathcal{C}[f]$ denotes the collision term. In terms of Ψ , the perturbation equation reads

$$\frac{d}{d\tau} \Psi(\tau, \mathbf{x}, q, \hat{q}) + \frac{\partial \ln \bar{f}(\tau, q)}{\partial q} \left(\frac{dq}{d\tau}\right)^{(1)} + \Psi(\tau, \mathbf{x}, q, \hat{q}) \frac{d \ln \bar{f}(\tau, q)}{d\tau} = \frac{1}{\bar{f}(\tau, q)} \mathcal{C}[f]^{(1)}, \quad (2.12)$$

where a superscript (1) denotes the perturbation to a given term. In most relevant scenarios we may drop the term proportional to $d\bar{f}/d\tau$, justified by noting that $dq/d\tau$ vanishes at the background level and assuming that the background distribution function is a function of q alone. The latter condition holds, e.g., for species in equilibrium and for collisionless, relativistic particles (like SM neutrinos after weak decoupling).

Generically, Ψ comprises scalar, vector, and tensor contributions, but only the latter sources gravitational waves. Expanding the \hat{q} -dependence of the distribution function in Fourier space as

$$\Psi(\tau, \mathbf{k}, q, \hat{q}) = \Psi^{(S)}(\tau, \mathbf{k}, q, \hat{q}) + \sum_{\lambda} \hat{q}_i \epsilon_i^\lambda(\mathbf{k}) \Psi_\lambda^{(V)}(\tau, \mathbf{k}, q, \hat{q}) + \sum_{\lambda} \hat{q}_i \hat{q}_j \epsilon_{ij}^\lambda(\mathbf{k}) \Psi_\lambda^{(T)}(\tau, \mathbf{k}, q, \hat{q}) \quad (2.13)$$

[with $\epsilon_i^\lambda(\mathbf{k})$ a suitable basis of transverse polarization vectors] defines the scalar-vector-tensor decomposition of Ψ that uniquely maps into those components that respectively source the scalar, vector, and tensor parts of Einstein's equations.² To linear order in perturbations, the part of the Boltzmann equation proportional to $\hat{q}_i \hat{q}_j \epsilon_{ij}^\lambda(\mathbf{k})$ is

$$\frac{\partial \Psi_\lambda^{(T)}}{\partial \tau} + ik\mu \frac{q}{\mathcal{E}} \Psi_\lambda^{(T)} - \frac{1}{2} \frac{\partial \ln \bar{f}}{\partial \ln q} h'_\lambda = \frac{1}{\bar{f}(q)} \mathcal{C}[f]_\lambda^{(T)}. \quad (2.14)$$

Here $\mu = \hat{k} \cdot \hat{q}$ is the cosine of the angle between the wavenumber \mathbf{k} and the propagation direction \mathbf{q} , and $\mathcal{C}[f]_\lambda^{(T)}$ denotes the tensor component of the (yet-to-be-specified) collision term. Because $dq/d\tau$ and $d\hat{q}/d\tau$ are themselves first order in perturbations (via the geodesic equation), the terms proportional to $\partial \Psi_\lambda^{(T)}/\partial q$ and $\partial \Psi_\lambda^{(T)}/\partial \hat{q}_i$ vanish at leading order.

²Seeing this requires observing in the geodesic equation that contributions from scalar, vector, and tensor perturbations to metric are each proportional to matching factors of \hat{q}_i , ϵ_i^λ , and ϵ_{ij}^λ . The linear-order Boltzmann equation may then be split into three independent equations on this basis. The scalar-vector-tensor decomposition of the stress-energy tensor [defined below in Eq. (2.18)] involves integrals over particle propagation directions weighted by various factors of \hat{q}_i which reveal that Eq. (2.13) also provides the relevant decomposition for the Einstein equations.

The angular (μ) dependence of the Boltzmann equation is most conveniently decomposed in a partial wave expansion, i.e., onto the orthogonal basis of Legendre polynomials, $P_l(\mu)$. This procedure recasts the Boltzmann equation into an infinite hierarchy of coupled equations for the moments of the distribution function. While one may substitute such an expansion for $\Psi_\lambda^{(T)}$ directly, our focus on relativistic species enables the q -dependence of the equations to be integrated out. We therefore define the moment expansion of the (suitably normalized) perturbations to the distribution function and the collision term as

$$F(\tau, \mathbf{k}, \hat{q}) \equiv \frac{\int dq q^3 \bar{f}(q) \Psi(\tau, \mathbf{k}, q, \hat{q})}{\int dq q^3 \bar{f}(q)} \equiv \sum_{l=0}^{\infty} (-i)^l (2l+1) F_l(\tau, \mathbf{k}) P_l(\mu) \quad (2.15)$$

and

$$C(\tau, \mathbf{k}, \hat{q}) \equiv \frac{\int dq q^3 \mathcal{C}[f]^{(1)}/\bar{f}(q)}{\int dq q^3 \bar{f}(q)} \equiv \sum_{l=0}^{\infty} (-i)^l (2l+1) C_l(\tau, \mathbf{k}) P_l(\mu). \quad (2.16)$$

Inserting this expansion into Eq. (2.14) yields the Boltzmann hierarchy,

$$\frac{\partial F_{\lambda,l}^{(T)}}{\partial \tau} - \frac{k}{2l+1} \left[l F_{\lambda,l-1}^{(T)} - (l+1) F_{\lambda,l+1}^{(T)} \right] + 2\delta_{l0} h'_\lambda = C_{\lambda,l}^{(T)}, \quad (2.17)$$

after also taking the relativistic limit, $\mathcal{E} \rightarrow q$.

Knowing the evolution of the phase-space density itself, we now compute the source to (the tensor part of) Einstein's equation. The stress-energy tensor of a species with phase-space density f is

$$T^\alpha{}_\beta(\tau, \mathbf{k}) = \frac{1}{\sqrt{-g}} \int dp_1 dp_2 dp_3 \frac{p^\alpha p_\beta}{p^0} f(\tau, \mathbf{k}, q, \hat{q}), \quad (2.18)$$

with p^α the conjugate momentum. For a relativistic species, the transverse-traceless component of the space-space perturbation $\delta T^i{}_j$, projected onto $\epsilon_{ij}^\lambda(\mathbf{k})$, is [70, 108]

$$\pi_\lambda^T(\tau, \mathbf{k}) = \bar{\rho}(\tau) \left(\frac{2}{15} F_{\lambda,0}^{(T)}(\tau, \mathbf{k}) + \frac{4}{21} F_{\lambda,2}^{(T)}(\tau, \mathbf{k}) + \frac{2}{35} F_{\lambda,4}^{(T)}(\tau, \mathbf{k}) \right). \quad (2.19)$$

The system of equations—Eq. (2.3) for h_λ and Eq. (2.17) for $F_{\lambda,l}^{(T)}$ —depend explicitly upon wavenumber only via the combination $k\tau \equiv x$. In terms of this dimensionless time coordinate, in Fourier space

$$\partial_x F_{\lambda,l}^{(T)} = \frac{1}{2l+1} \left[l F_{\lambda,l-1}^{(T)} - (l+1) F_{\lambda,l+1}^{(T)} \right] - 2\delta_{l0} \partial_x h_\lambda + \frac{1}{k} C_{\lambda,l}^{(T)} \quad (2.20a)$$

and

$$\partial_x^2 h_\lambda = -2 \frac{\partial_x a}{a} \partial_x h_\lambda - h_\lambda + 6\Omega_\nu(\tau) \left(\frac{\partial_x a}{a} \right)^2 \left(\frac{2}{15} F_{\lambda,0}^{(T)} + \frac{4}{21} F_{\lambda,2}^{(T)} + \frac{2}{35} F_{\lambda,4}^{(T)} \right). \quad (2.20b)$$

The fraction of energy in the relativistic species under consideration is $\Omega_\nu(\tau) \equiv \bar{\rho}_\nu(\tau)/\bar{\rho}(\tau)$, suggestively labeled by ν (though we use this definition for any relativistic species under consideration, not just Standard Model neutrinos). Note that $\Omega_\nu(\tau)$ does not necessarily denote the fraction of energy in particles that are specifically collisionless or free streaming at τ —in interacting scenarios, the species ν (or some fraction thereof) may be fluidlike when its interactions are efficient. In fully noninteracting scenarios, we refer to the fraction of energy in species that are specifically free-streaming with f_{fs} .

All that remains is to specify the background evolution of the Universe. In a Universe dominated by a single component with equation of state w , the solution to the Friedmann equations is

$$\frac{a(\tau)}{a(\tau_i)} = \left(\frac{\tau}{\tau_i} \right)^\alpha \quad (2.21a)$$

$$\mathcal{H}(\tau) = \frac{\alpha}{\tau}, \quad (2.21b)$$

where $\alpha = 2/(1 + 3w)$. In this case, $\partial_x a/a = \alpha/x$. In a radiation Universe with $\alpha = 1$, $\Omega_\nu(\tau)$ is constant, barring decay channels into or of the species ν . The neutrinos' share of the radiation energy (in the SM) is

$$R_\nu^{\text{SM}} \equiv \frac{\bar{\rho}_\nu}{\bar{\rho}_\gamma + \bar{\rho}_\nu}. \quad (2.22)$$

For N_ν neutrino species, after electron-positron annihilation R_ν^{SM} is

$$R_\nu^{\text{SM}} = \left[1 + \left(\frac{11}{4} \right)^{4/3} \frac{8}{7N_\nu} \right]^{-1}, \quad (2.23)$$

taking the value $R_\nu^{\text{SM}} \approx 0.40523$ for $N_\nu = 3$ neutrino species. When considering more general early-Universe scenarios, the free-streaming abundance f_{fs} may be treated as a free parameter.

More generally, we may employ the analytic solution for a matter-radiation Universe,

$$\frac{a(\tau)}{a(\tau_{\text{eq}})} = \frac{y}{8} \left(y + 4\sqrt{2} \right) \quad (2.24)$$

where $y = k_{\text{eq}}\tau$ and $k_{\text{eq}} \equiv \mathcal{H}(\tau_{\text{eq}}) \approx 10^{-2} \text{Mpc}^{-1}$ [13] is the horizon scale evaluated at matter-radiation equality. This scale corresponds to a present-day frequency $f_{\text{eq}} = 1.55 \times 10^{-17} \text{Hz}$. Note that $k_{\text{eq}}\tau_{\text{eq}} = 4 - 2\sqrt{2} \approx 1.17$ and

$$\frac{\mathcal{H}(\tau)}{k_{\text{eq}}} = \frac{\partial_y a}{a} = \frac{4\sqrt{2} + 2y}{4\sqrt{2}y + y^2}. \quad (2.25)$$

In this case, Eq. (2.20) depends on the ratio k/k_{eq} , both via the change in the expansion rate and because the neutrino abundance begins to decrease as the Universe enters matter domination. At all times after electron-positron annihilation,

$$\Omega_\nu(\tau) = \frac{R_\nu^{\text{SM}}}{1 + a(\tau)/a(\tau_{\text{eq}})}. \quad (2.26)$$

This background solution (neglecting dark energy) is sufficiently accurate to study the effect of free-streaming radiation on all observable scales: the Universe expands by a factor more than 10^3 by dark-energy–matter equality, with a correspondingly large reduction in $\Omega_\nu(\tau)$ [via Eq. (2.26)] and thereby also the effect of free-streaming neutrinos on gravitational waves.

2.2 Modeling interacting radiation

The elusiveness of neutrinos positions them as a prime candidate portal to dark sectors and physics beyond the Standard Model. Abundant motivations for novel interactions amongst the SM neutrinos include mechanisms for their masses, extensions to the SM gauge sector, and the possibility of sterile neutrino dark matter (see Refs. [109, 110] for recent reviews). Extensive literature has considered the cosmological signatures of neutrino self-interactions [79–84, 111–137], neutrino interactions with dark matter [138–144], and interacting dark sectors more generally [75, 76, 145–163]. A substantial amount of interest in these models is due to their potential to alleviate tensions in measurements of the Hubble constant [164] and the amplitude of matter fluctuations—e.g., Refs. [78, 79, 84, 130, 132, 134, 152, 153, 157, 161, 162, 165–176].

We now discuss the implementation of neutrino interactions (or that of other relativistic species), i.e., the form of the collision term in the Boltzmann equation. Under the assumption that the phase space perturbations are independent of momentum, the full (momentum-dependent) collision term integrates to [82]

$$C_{\lambda,l} = \alpha_l \partial_\tau \kappa_\nu F_{\lambda,l}. \quad (2.27)$$

Here κ_ν is the optical depth of the species ν (and $\partial_\tau \kappa_\nu$ the time-dependent interaction rate), and the α_l are numerical coefficients that arise when computing the moments of the full collision term. This treatment is also referred to as the relaxation time approximation. Ref. [82] implemented the exact (momentum-dependent) scalar Boltzmann hierarchy and the momentum-integrated hierarchy using Eq. (2.27) for the case of 2 – 2 neutrino scattering mediated by a heavy scalar, finding that the dynamics of the neutrino fluid variables and the resulting CMB angular power spectra agree extremely well between the two approaches. A possible explanation for this result is that gravitational consequences of neutrinos (which are the only cosmologically relevant ones after the weak interactions decouple) are themselves momentum-integrated quantities and therefore are not sensitive to neutrino spectral distortions [80].

While the validity of Eq. (2.27) has not been demonstrated for, e.g., neutrino interactions via a light mediator, nor explicitly for the tensor hierarchy under study here, we assume it provides a sufficient approximation to capture the transition from fluidlike to free-streaming behavior. Furthermore, Ref. [82] computed the coefficients α_l for the scalar Boltzmann hierarchy directly from the exact collision integral. Energy and momentum conservation require that α_0 and α_1 vanish, while the values for larger multipoles rise from $\alpha_2 = 0.40$ to $\alpha_l = 0.48$ for $l \geq 6$. Noting that there is no conservation equation for tensors (i.e., the linear-order part of the energy-momentum conservation equation, $\nabla_\mu T^{\mu\nu} = 0$, has no tensor component), we take $\alpha_l = 1$ for all l ; their exact values would only amount to an order unity change in the relationship between the neutrino interaction rate and the time of de-/recoupling.

For generality's sake, we parameterize the interaction rate with temperature dependence of the form

$$\partial_\tau \kappa_\nu(\tau) = -\frac{a(\tau)}{a(\tau_\star)} \lambda T_\nu(\tau)^n \quad (2.28)$$

in terms of an effective coupling constant λ (with mass dimension $1 - n$), with $a(\tau_\star)$ the scale factor at the time of the decoupling/recoupling transition. Interactions are efficient when their rate is larger than the expansion rate, so $|\partial_\tau \kappa_\nu(\tau_\star)| = \mathcal{H}(\tau_\star)$ marks the time of the transition. Since both the comoving Hubble rate and the temperature decay as $1/a(\tau)$ in the radiation era, decoupling occurs for scenarios with $n > 2$ and recoupling when $n < 2$. Self-interactions mediated by heavy and light degrees of freedom, for example, respectively have $n = 5$ and $n = 1$. See Ref. [86] for a similar phenomenological approach applied to the effect of neutrinos interactions on the CMB and large-scale structure.³

The de-/recoupling transition modulates the magnitude of the damping effect on scales near the horizon at that time, $k_\star \equiv \mathcal{H}(\tau_\star)$. In terms of this scale, we may write

$$\partial_\tau \kappa_\nu(\tau) = -\frac{\lambda T_\nu(\tau_\star)^n}{[a(\tau)/a(\tau_\star)]^{n-1}} = -k_\star \left(\frac{a(\tau)}{a(\tau_\star)} \right)^{1-n}, \quad (2.29)$$

assuming that the neutrino temperature decays as $1/a(\tau)$ at all times. We can replace the dependence on $a(\tau_\star)$ with k/k_\star as follows. First write the Friedmann equation in terms of the neutrino temperature and fraction $\Omega_\nu(\tau)$ [given by Eq. (2.26)] as

$$\mathcal{H}(\tau) = \sqrt{\frac{a(\tau)^2 \bar{\rho}_\nu(\tau)}{3M_{\text{pl}}^2 \Omega_\nu(\tau)}} = \sqrt{\frac{7\pi^2}{120\Omega_\nu(\tau)M_{\text{pl}}^2} \frac{T_\nu(\tau_\star)^2}{a(\tau)/a(\tau_\star)}}, \quad (2.30)$$

with six effective neutrino degrees of freedom. Taking the ratio of the above evaluated at τ and τ_\star leads to

$$\frac{a(\tau)}{a(\tau_\star)} = \sqrt{\frac{\Omega_\nu(\tau_\star)}{\Omega_\nu(\tau)} \frac{k_\star}{\mathcal{H}(\tau)}}. \quad (2.31)$$

³Beyond interaction rates with power-law dependence on the temperature, Ref. [86] also considers transiently efficient interactions motivated by models featuring neutrino decay and inverse decay. In these scenarios the interaction rate, rather than changing monotonically, increases to some maximum and subsequently decreases with time. For simplicity, we restrict our results to those of the form Eq. (2.28).

Plugging Eq. (2.31) into Eq. (2.29) with $\tau = \tau_k \equiv 1/k$ yields

$$\partial_\tau \kappa_\nu(\tau) = -k \left(\frac{a(\tau)}{a(\tau_k)} \right)^{1-n} \left(\frac{k}{k_\star} \right)^{n-2} \left(\frac{\Omega_\nu(\tau_k)}{\Omega_\nu(\tau_\star)} \right)^{\frac{n-1}{2}}. \quad (2.32)$$

When horizon crossing (τ_k) and de-/recoupling (τ_\star) are both sufficiently early compared to equality (τ_{eq}) but still after weak decoupling and e^+e^- annihilation, the ratio of the neutrino abundances is unity. In a radiation Universe,

$$\partial_\tau \kappa_\nu(\tau) = -k (k\tau)^{1-n} \left(\frac{k}{k_\star} \right)^{n-2}. \quad (2.33)$$

Choosing instead to use Eq. (2.31) with $\tau = \tau_{\text{eq}}$ yields

$$\partial_\tau \kappa_\nu(\tau) = -k_{\text{eq}} \left(\frac{a(\tau)}{a(\tau_{\text{eq}})} \right)^{1-n} \left(\frac{k_{\text{eq}}}{k_\star} \right)^{n-2} \left(\frac{\Omega_\nu(\tau_{\text{eq}})}{\Omega_\nu(\tau_\star)} \right)^{\frac{n-1}{2}}. \quad (2.34)$$

Note that $\Omega_\nu(\tau)/\Omega_\nu(\tau_{\text{eq}}) \approx 2$ at times τ deep in the radiation era. Lastly, using

$$\kappa(\tau_1, \tau_2) \equiv \int_{\tau_1}^{\tau_2} d\tilde{\tau} \partial_{\tilde{\tau}} \kappa_\nu(\tilde{\tau}) \quad (2.35)$$

as shorthand notation, we define the opacity function

$$\mathcal{O}_\nu(\tau_1, \tau_2) = 1 - e^{\kappa(\tau_1, \tau_2)}, \quad (2.36)$$

which characterizes the probability that a single particle free streams between times τ_1 and τ_2 .

2.3 Integral solutions

Before obtaining numerical results, we turn to formal, integral solutions for approximate, analytic solutions and intuition. Such integral equations were derived in Ref. [177] for scalar, vector, and tensor perturbations sourced by collisionless particles. Ref. [177] also outlined the procedure to obtain analytic solutions in series of spherical Bessel functions (eventually further developed by Refs. [178–180]), anticipating that free-streaming matter would damp metric perturbations. Ref. [181] (and also Ref. [182]) employed an alternative power series solution and appears to have been the first to present results for tensor perturbations, finding a damping in amplitude of order 0.6 for free-streaming-only solutions compared to fluid-only ones, consistent with results here and elsewhere. Refs. [70, 108] derived and applied this formalism to the neutrino content of the Universe (after decoupling of the weak interactions) in the standard Big Bang model.

Refs. [70, 177, 181, 182] (and subsequent work) recast the coupled system of equations Eq. (2.20) into a single integro-differential equation, exchanging the anisotropic stress's dependence on the distribution function for an integral over the history of the gravitational wave itself. To obtain this result, return to the momentum-integrated Boltzmann equation (before decomposing into partial waves), Eq. (2.14), which with Eq. (2.16) defining the collision term takes the form

$$0 = \partial_x F_\lambda^{(T)}(x, \mu) + i\mu F_\lambda^{(T)}(x, \mu) - \partial_x \kappa_\nu(x) F_\lambda^{(T)}(x, \mu) + 2\partial_x h_\lambda(x). \quad (2.37)$$

Observe that Eq. (2.37) has the formal solution (from some initial condition at x_i)

$$F_\lambda^{(T)}(x, \mu) = e^{-i\mu(x-x_i) + \kappa_\nu(x_i, x)} F_\lambda^{(T)}(x_i, \mu) - 2 \int_{x_i}^x du e^{\kappa_\nu(u, x)} e^{-i\mu(x-u)} \partial_u h_\lambda(u). \quad (2.38)$$

Replacing the exponential inside the integral with the partial wave expansion of a plane wave and recomputing the anisotropic stress [Eq. (2.19)], the gravitational wave equation of motion becomes

$$\partial_x^2 h_\lambda + 2 \frac{\partial_x a}{a} \partial_x h_\lambda + h_\lambda = -24\Omega_\nu(\tau) \left(\frac{\partial_x a}{a} \right)^2 \int_{x_i}^x du [1 - \mathcal{O}_\nu(u, x)] K(x-u) \partial_u h_\lambda, \quad (2.39)$$

where we take the initial condition $F_\lambda^{(T)}(x_i, \mu) = 0$ and define

$$K(y) \equiv \frac{1}{15}j_0(y) + \frac{2}{21}j_2(y) + \frac{1}{35}j_4(y) = \frac{j_2(y)}{y^2} \quad (2.40)$$

in terms of the spherical Bessel functions of the first kind $j_\gamma(x)$. Equation (2.39) reproduces the form obtained in Ref [70] for the collisionless case, $\mathcal{O}_\nu(u, x) = 0$. Integro-differential equations like Eq. (2.39) may be solved numerically via an iterative algorithm or by discretizing in time and solving the resulting linear system. Alternatively, Eq. (2.39) may be solved analytically in a series of spherical Bessel functions, as applied to the case of inflationary gravitational waves (and collisionless neutrinos) in Refs. [178–180].

Though the source term in the integro-differential form Eq. (2.39) depends upon h_λ itself, it proves useful nonetheless to study the formal solution in terms of Green functions. First, define the rescaled tensor perturbation $v_\lambda \equiv ah_\lambda$, which does not decay with the expansion of the Universe. The gravitational wave equation of motion Eq. (2.3) in Fourier space takes the form

$$v_\lambda''(\tau, \mathbf{k}) + \left(k^2 - \frac{a''}{a}\right)v_\lambda(\tau, \mathbf{k}) = a \frac{2a^2}{M_{\text{pl}}^2} \pi_\lambda^T(\tau, \mathbf{k}). \quad (2.41)$$

For simplicity, we here fix a single-component Universe [Eq. (2.21)] at the background level and again work in terms of the coordinate $x \equiv k\tau$. The particular solution to Eq. (2.41) is a convolution of the source and the Green function $G(x; \tilde{x})$ that satisfies

$$\partial_x^2 G(x, \tilde{x}) + \left(1 - \frac{\alpha(\alpha - 1)}{x^2}\right) G(x, \tilde{x}) = \delta(x - \tilde{x}). \quad (2.42)$$

The causal solution is

$$G(x; \tilde{x}) = \Theta(x - \tilde{x})x\tilde{x} [j_{\alpha-1}(\tilde{x})y_{\alpha-1}(x) - j_{\alpha-1}(x)y_{\alpha-1}(\tilde{x})], \quad (2.43)$$

where Θ is the Heaviside function and j_γ and y_γ are the order- γ spherical Bessel functions of the first and second kind, respectively. Denoting the homogeneous solution as $h_\lambda^{(0)}(x)$ and substituting $a(\tau) = (k\tau)^\alpha$, the full (homogeneous plus particular) solution reads

$$h_\lambda(x) = h_\lambda^{(0)}(x) + \frac{1}{x^\alpha} \int_{x_i}^x d\tilde{x} G(x; \tilde{x}) \tilde{x}^\alpha \frac{2\tilde{x}^{2\alpha}}{k^2 M_{\text{pl}}^2} \pi_\lambda^T(\tilde{x}). \quad (2.44)$$

We are mainly interested in the radiation era, in which $\alpha = 1$ and the Green function is

$$G(x; \tilde{x}) = \sin x \cos \tilde{x} - \sin \tilde{x} \cos x = \sin(x - \tilde{x}). \quad (2.45)$$

Finally, plugging in the integral solution for π_λ^T as in Eq. (2.39) and taking Ω_ν constant yields

$$h_\lambda(x) = h_\lambda^{(0)}(x) - \frac{24\Omega_\nu}{x} \int_{x_i}^x d\tilde{x} \frac{\sin(x - \tilde{x})}{\tilde{x}} \int_{x_i}^{\tilde{x}} du [1 - \mathcal{O}_\nu(u, \tilde{x})] K(\tilde{x} - u) \partial_u h_\lambda(u). \quad (2.46)$$

Since $K(y) \approx -\sin(y)/y^3$ for $y \gg 1$, at late times the integral over u receives most of its support where $u \sim \tilde{x}$. The contributions to the inhomogeneous term from late times (relative to horizon crossing) are therefore suppressed, localizing the importance of anisotropic stress near horizon crossing. As such, stochastic backgrounds of gravitational waves encode the interaction history of relativistic species. Though Eq. (2.46) does not permit a solution by direct integration, we might hope to gain insight by approximating $\partial_u h_\lambda(u)$ with the homogeneous solution (i.e., to zeroth order in an expansion in Ω_ν). We explore the utility of this approach in application to inflationary gravitational waves in Section 3.1.

We close by connecting the above formalism to the observable gravitational wave spectrum. We first phrase the formal solution in terms of a modulation of the amplitude and phase of the solution as

induced by free-streaming particles. Decompose the solution Eq. (2.46) onto sine and cosine modes [i.e., using the first form of Eq. (2.45)] as

$$h_\lambda(x) \equiv h_{\lambda,s}(x) \frac{\sin(x)}{x} + h_{\lambda,c}(x) \frac{\cos(x)}{x} \quad (2.47)$$

$$\equiv [h_{\lambda,s} + \mathcal{I}_s(x)] \frac{\sin(x)}{x} + [h_{\lambda,c} + \mathcal{I}_c(x)] \frac{\cos(x)}{x}, \quad (2.48)$$

where $h_{\lambda,s}$ and $h_{\lambda,c}$ parameterize the homogeneous solution while the inhomogeneous contributions are

$$\begin{pmatrix} \mathcal{I}_s(x) \\ \mathcal{I}_c(x) \end{pmatrix} \equiv 24\Omega_\nu \int_{x_i}^x d\tilde{x} \frac{1}{\tilde{x}} \begin{pmatrix} -\cos \tilde{x} \\ \sin \tilde{x} \end{pmatrix} \int_{x_i}^{\tilde{x}} du [1 - \mathcal{O}_\nu(u, \tilde{x})] K(\tilde{x} - u) \partial_u h_\lambda(u). \quad (2.49)$$

Comparing Eq. (2.47) to

$$h_\lambda(x) \equiv A(x) \frac{\sin[x + \varphi(x)]}{x} \quad (2.50)$$

reveals that the (time-dependent) amplitude and phase of the solution are respectively modulated by free-streaming particles as

$$A(x) = \sqrt{h_{\lambda,s}(x)^2 + h_{\lambda,c}(x)^2} \quad (2.51)$$

$$\varphi(x) = \arctan\left(\frac{h_{\lambda,c}(x)}{h_{\lambda,s}(x)}\right). \quad (2.52)$$

Parametrizing in terms of an amplitude and phase is valid at all times only in a radiation-dominated Universe. In any single-component Universe, however, Eq. (2.50) is still valid asymptotically, since the late-time limits of spherical Bessel functions of any order are proportional to sine and cosine. We therefore define $A_\infty \equiv A(\infty)$ and $\varphi_\infty \equiv \varphi(\infty)$. [Note as well that $A_\infty[f_{\text{fs}} = 0] = h_{\lambda,0}$ only in a radiation dominated Universe; for general α the value is $2^\alpha \Gamma(\alpha + 1/2) h_{\lambda,0} / \sqrt{\pi}$.]

We present main results in terms of the relative change to the spectral energy density in gravitational waves [Eq. (2.7)],

$$\frac{\Omega_{\text{GW}}}{\Omega_{\text{GW}}[f_{\text{fs}} = 0]} = \left(\frac{A_\infty}{A_\infty[f_{\text{fs}} = 0]} \right)^2, \quad (2.53)$$

compared to a Universe with a free-streaming fraction $f_{\text{fs}} = 0$ (and therefore no anisotropic stress). The phase shift is likely unobservable for direct detection of the strain of stochastic backgrounds, which average signals over an integration time much longer than the gravitational-wave period. However, phase shifts would impact the spectrum of CMB polarization, since the visibility function for photons is sharply peaked at recombination (making the CMB an effective snapshot of that moment in time).

3 Damping of inflationary gravitational waves

We now apply the formalism established in Section 2 to develop a semianalytic understanding of the effect of relativistic particles on the primordial gravitational wave background generated during inflation. Using the formal results of Section 2.3, in Section 3.1 we study the amplitude modulation and phase shift of gravitational waves due to free-streaming particles. Building on intuition from these semianalytic results in noninteracting scenarios, Section 3.2 presents numerical results for a variety of scenarios in which interactions decouple or recouple, focusing on the effect of SM neutrinos.

3.1 Results in noninteracting scenarios

Gravitational waves generated during inflation exit the horizon in the asymptotic past and remain frozen until their wavelength reenters the horizon. This case corresponds to an initial condition far

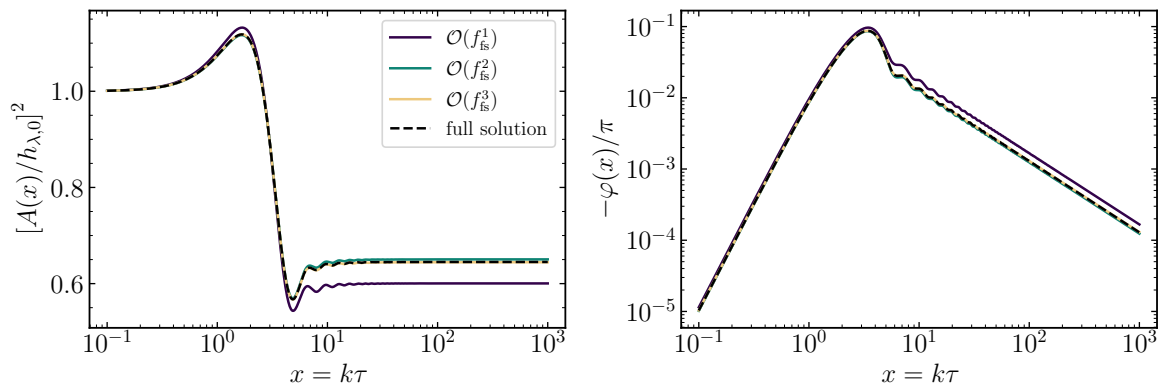


Figure 1. Time dependent amplitude and phase, Eqs. (2.51) and (2.52), in the presence of free-streaming radiation. The solid curves depict the semianalytic results at varying orders in f_{fs} , while the black dashed curve shows the quantities evaluated with a full solution to the Boltzmann hierarchy. All results fix the free-streaming fraction to that of SM neutrinos, $f_{\text{fs}} = R_{\nu}^{\text{SM}} = 0.40523$.

outside the horizon ($x = k\tau = k/\mathcal{H} \ll 1$) of

$$\lim_{k\tau \rightarrow 0} h_{\lambda}(x) = h_{\lambda,0} \quad (3.1a)$$

$$\lim_{k\tau \rightarrow 0} \partial_x h_{\lambda,0}(x) = 0 \quad (3.1b)$$

$$\lim_{k\tau \rightarrow 0} F_{\lambda,l}^{(T)}(x) = 0 \quad (3.1c)$$

in terms of the primordial amplitude $h_{\lambda,0}$. The homogeneous solution (i.e., in the absence of anisotropic stress) to Eq. (2.3) is $h_{\lambda}^{(0)}(x) = h_{\lambda,0} j_0(x) = h_{\lambda,0} \sin x/x$. In the language of Eq. (2.47), $h_{\lambda,s} = h_{\lambda,0}$ and $h_{\lambda,c} = 0$.

As argued in Section 2.3, the impact of free-streaming particles decays with time. In practice, this means that $A(x)$ and $\varphi(x)$ converge⁴ to their late-time values A_{∞} and φ_{∞} relatively quickly; in Appendix B we show that, at late times $x \gg 1$,

$$\left(\frac{A(x)}{h_{\lambda,0}}\right)^2 \approx \left(1 - \frac{5}{9}f_{\text{fs}}\right)^2 + \frac{f_{\text{fs}}^2 - 2f_{\text{fs}}(1 - 5f_{\text{fs}}/9)\sin^2 x}{x^2} \quad (3.2a)$$

$$\varphi(x) \approx -\frac{1}{x} \frac{f_{\text{fs}}}{1 - 5f_{\text{fs}}/9} \quad (3.2b)$$

when inserting the homogeneous solution $h_{\lambda}^{(0)}$ into the integrals in Eq. (2.49) (and replacing Ω_{ν} with f_{fs}). We display the full result for all times x in Fig. 1, which shows for comparison the result from a full numerical solution to the Boltzmann hierarchy (as described in Appendix A).⁵ While the semianalytic results for \mathcal{I}_s and \mathcal{I}_c are simply proportional to f_{fs} , the amplitude and phase depend nonlinearly on f_{fs} , for which reason Fig. 1 fixes $f_{\text{fs}} = R_{\nu}^{\text{SM}}$ for SM neutrinos after weak decoupling. As one might anticipate by the form of Eq. (2.51), the overall amplitude of gravitational waves is in fact enhanced just after horizon crossing due to the sourcing of the cosine mode (which is not present in the absence of anisotropic stress). The sine mode is initially enhanced as well, but $\mathcal{I}_s(x)$ begins decreasing rapidly from its maximum just before $|\mathcal{I}_c|$ (and also the phase shift) is maximized. The amplitude rapidly

⁴Within the present framework, there is no means by which the tensor anisotropic stress π_{λ}^T can grow with time (or remain constant), so the integrals are convergent. The tensor anisotropic stress would grow, if, for example, another species decays into relativistic particles or directly sources gravitational waves.

⁵Figure 1 also displays results at higher orders in the expansion in f_{fs} , i.e., those obtained by successively inserting solutions into Eq. (2.46) and computing integrals by numerical quadrature. The iterative procedure quickly converges to the fully numerical result. A similar approach was recently applied to scalar perturbations in Refs. [183, 184].

drops during the first oscillation and then begins to oscillate as $\sin^2 x/x^2$ about its asymptotic value, as per Eq. (3.2a). At the same time, the phase decays linearly as in Eq. (3.2b). See Ref. [185] for an alternative derivation of these results using real-space Green function methods.

Finally, we comment on the damping factor’s dependence on f_{fs} . The aforementioned analytic, series solution to Eq. (2.39) [178–180] was employed in Ref. [65] to compute an analytic approximation to the damping factor for inflationary gravitational waves that is accurate to 0.1% for all f_{fs} between 0 and 1. Our numerical solutions to Eq. (2.20) [with the initial condition Eq. (3.1)] verify the accuracy of the analytic approximation of Ref. [65] over the full range of f_{fs} between 0 and 1. However, by numerological coincidence, the (far simpler) fitting function

$$\frac{A_\infty}{A_\infty[f_{\text{fs}}=0]} = \left(1 + \frac{f_{\text{fs}}}{9} + \frac{f_{\text{fs}}^2}{23}\right) e^{-2f_{\text{fs}}/3} \quad (3.3)$$

reproduces numerical results to one part in 10^4 for all f_{fs} . This fitting formula, to leading order in f_{fs} , agrees with the semianalytic result of (the square root of) Eq. (3.2a), $1 - 5f_{\text{fs}}/9$.

3.2 Results in interacting scenarios

Having reviewed the known effects of free-streaming particles on gravitational waves, we turn to more general scenarios in which relativistic species transition between weakly and strongly interacting states. We first establish expectations based upon the semianalytic results of Section 3.1, inferring from Eq. (3.2) and Fig. 1 how the instantaneous decoupling or recoupling of interactions would modulate the gravitational wave power spectrum.

Consider first dark radiation that decouples from interactions. For wavenumbers k much smaller than the horizon size at the transition k_* , decoupling occurs at $x_* = k\tau_* \ll 1$, well before horizon crossing; these modes therefore experience the full damping effect. In the opposite case, free streaming is postponed until well after horizon crossing—beyond when the bulk of the damping effect would take place. A residual phase shift and amplitude suppression occur respectively at linear and quadratic order in k_*/k , evident by inspecting the integrands of Eq. (2.49). For modes entering the horizon near the time of decoupling, the results are more complex. For example, some modes do not experience the initial enhancement of the cosine mode (and the overall amplitude), and could therefore be *more* suppressed than modes that enter the horizon well after decoupling. The decaying oscillations in time in Eq. (3.2a) would imprint a relic amplitude oscillation (in k) for modes that begin oscillating slightly sooner before decoupling. Indeed, this exact oscillatory effect for neutrino decoupling from the weak interactions was observed in Refs. [68, 186] and (correctly) attributed to use of the instantaneous decoupling approximation. In reality, decoupling (for interaction rates proportional to, e.g., T^5) takes a nonvanishing amount of time, smearing out such features; however, they may be evident in scenarios where decoupling occurs due to a rapid drop in number density, such as dark hydrogen recombination.

A similar analysis of Fig. 1 for recoupling scenarios suggests that modes that reenter the horizon near the time of recoupling would be slightly *enhanced*, since interactions would rapidly suppress anisotropic stress before the bulk of the amplitude suppression occurs. These modes would also retain a nonzero phase shift. The effect for modes with wavenumbers larger than k_* would be truncated: the amplitude is damped by an increasing amount with increasing k , saturating at the value for the noninteracting case, and the late-time phase shift approaches zero linearly with k_*/k .

Expectations in hand, we now present numerical solutions to Eq. (2.20). Rather than employing an iterative method to solve the integro-differential form of the system, we find it simple and efficient enough to solve the original system of equations [i.e., Eq. (2.20) for the gravitational waves and the Boltzmann hierarchy] directly using standard methods for ordinary differential equations. We outline our numerical implementation in Appendix A.

We first consider a radiation Universe (a suitable approximation for de-/recoupling occurring sufficiently early before matter-radiation equality, i.e., $k_* \gg k_{\text{eq}}$). Figure 2 displays the amplitude modulation relative to that for a Universe with no free-streaming radiation ($f_{\text{fs}} = 0$) for interaction rates with varying temperature dependence T^n . For comparison, Fig. 2 includes curves representing the instantaneous de-/recoupling cases (approximated with $n = \pm 25$ solutions for numerical convenience), which exhibit the oscillatory feature anticipated from Fig. 1 (and observed in, e.g., Refs. [68, 186]).

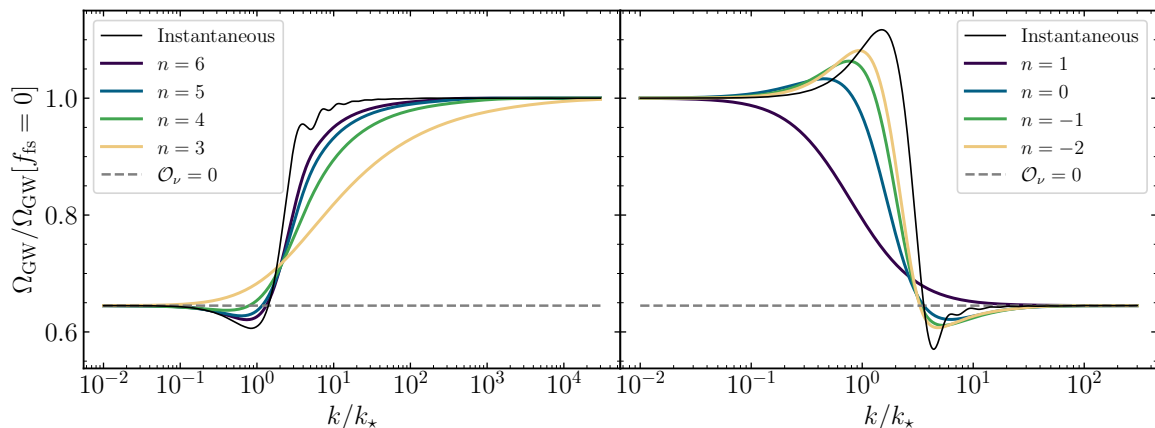


Figure 2. Damping factor (in a radiation Universe) for inflationary gravitational waves in decoupling (left) and recoupling (right) scenarios with interaction rates of varying temperature dependence T^n [Eq. (2.28)] as denoted by the legends (colored curves). The spectrum is normalized relative to that for a Universe with no free-streaming particles, and k_* denotes the horizon size at the time of de-/recoupling. The dashed grey curve depicts the result in the noninteracting case (i.e., zero opacity at all times), and the thin black curve that for instantaneous de-/recoupling. All results fix the abundance of the radiation sector to that of SM neutrinos, $\Omega_\nu = R_\nu^{\text{SM}} = 0.40523$.

(Note that the $n = 5$ curve corresponds to the result for standard neutrino decoupling, i.e., when the weak interactions become inefficient.) Results in all cases exhibit the nearly sigmoidal behavior expected from the preceding discussion, centered on some scale near k_* . Additionally, in scenarios where de-/recoupling occurs rapidly enough ($|n - 2| > 1$), we also observe the anticipated overshoot: modes which enter the horizon just after decoupling (or before recoupling) are damped more than in the noninteracting case. Furthermore, in the recoupling scenario modes with wavenumber close to k_* are indeed enhanced via the sourcing of the cosine mode.

To study scenarios relevant to the CMB, we adopt a matter-radiation Universe and consider $n = 5$ and 1 as benchmark decoupling and recoupling cases. Figure 3 displays results for scenarios of varying coupling strengths (phrased as usual in terms of the horizon size at de-/recoupling in units of Mpc^{-1} .) For the decoupling case, the interplay between the transition to free streaming and the onset of matter domination [which reduces the neutrino abundance per Eq. (2.26)] introduces a dip-like feature in the gravitational wave power spectrum. In recoupling scenarios, the reintroduction of interactions introduces a similar feature as the transition to matter domination, but at smaller scales. When recoupling occurs near matter-radiation equality, the two effects conspire to mildly enhance the gravitational wave spectrum on scales slightly larger than the horizon at equality.

Finally, the above results extend straightforwardly if only some fraction $F_{\text{interacting}}$ of the relativistic species self-interacts. In light of CMB constraints on the amount of energy in radiation (i.e., neutrinos) that can be fluidlike [75, 78, 155] as well as laboratory constraints on neutrino self-interactions (see, e.g., Ref. [166]), such scenarios are more probable (if neutrino interactions remain important during the formation of the CMB⁶). Figure 4 displays results for benchmark decoupling and recoupling scenarios, demonstrating that the damping before decoupling (or after recoupling) corresponds to the expectation for a Universe with a fraction $(1 - F_{\text{interacting}})\Omega_\nu$ of energy in free-streaming, relativistic particles. Analogous results would apply to dark radiation sectors, but the effect would be proportionally smaller (given cosmological constraints on new light relics).

⁶However, *Planck* and ACT polarization data appear to drive differing preferences for strongly interacting neutrinos; see Ref. [85] for a recent investigation. *Planck* constraints on strongly interacting neutrinos are also weaker when only one or two eigenstates interact [79, 84].

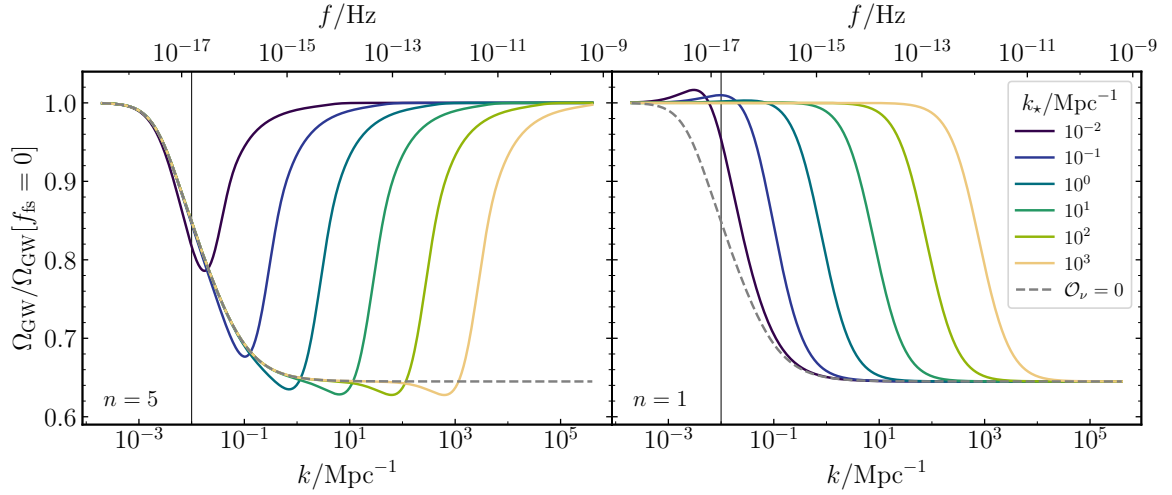


Figure 3. Impact of varying the epoch of de-/recoupling on the amplitude of inflationary gravitational waves. The damping factor for interactions mediated by heavy ($n = 5$, left) and light ($n = 1$, right) degrees of freedom are plotted for various coupling strengths parameterized in terms of the horizon scale k_* at the time of de-/recoupling, denoted by the legend. The dashed grey line depicts the result for neutrinos with no beyond-the-SM interactions. Vertical lines mark the horizon scale at matter-radiation equality; the abundance of neutrinos, and therefore the damping of gravitational waves, decays as matter comes to dominate the Universe’s energy budget. All results fix the abundance of the radiation sector to that of SM neutrinos, $\Omega_\nu = R_\nu^{\text{SM}} = 0.40523$.

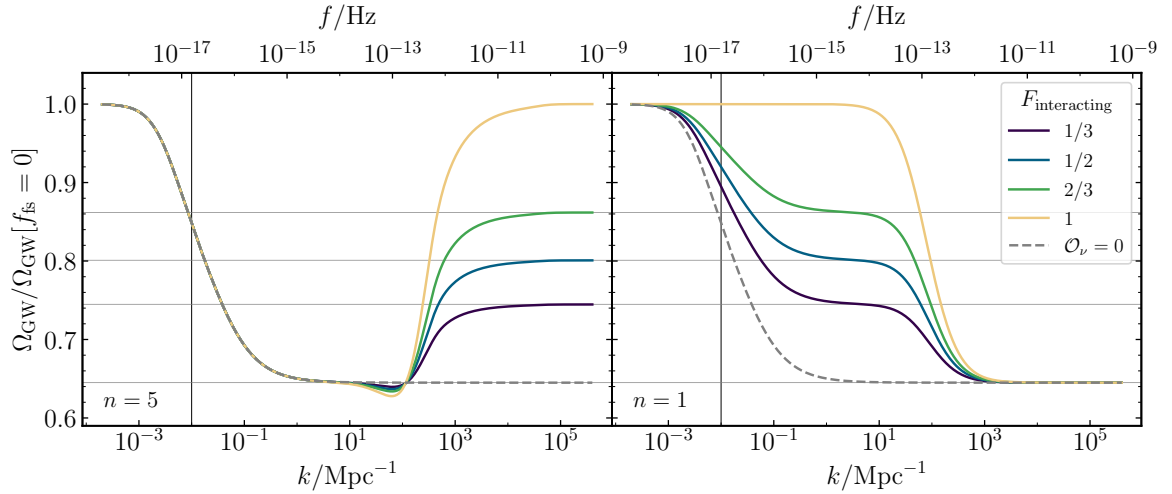


Figure 4. Damping factor for inflationary gravitational waves as a function of scale when a differing number of the neutrino eigenstates participate in interactions mediated by heavy ($n = 5$, left) and light ($n = 1$, right) degrees of freedom. All results take the horizon scale at the time of de-/recoupling to be $k_* = 10^2 \text{ Mpc}^{-1}$ and fix Ω_ν to the Standard Model value, $R_\nu^{\text{SM}} = 0.40523$, of which only a fraction $F_{\text{interacting}}$ (labeled by the legend) comprises interacting species. A curve assuming that effectively half of the neutrinos interact is included for illustrative purposes. Horizontal lines indicate the squared damping factors [evaluated with the fitting function Eq. (3.3)] for each case when taking $f_{\text{is}} = F_{\text{interacting}} \Omega_\nu$. The vertical lines indicate the horizon scale at matter-radiation equality.

4 Damping of causal gravitational waves

In contrast to inflation, which sources gravitational waves that remain frozen until they eventually reenter the horizon, most other cosmological sources of stochastic backgrounds (such as phase transitions or resonant particle production) occur sufficiently far inside the horizon that the effect of free-streaming particles is unimportant. On the other hand, in these scenarios the gravitational wave source is typically quadratic in some degree of freedom carrying anisotropic stress (e.g., the velocity of a fluid, the gradient of a scalar field, or electric and magnetic fields), coupling long-wavelength gravitational waves to the subhorizon, “causal” dynamics of the source. Ref. [88] provided a model-independent description of the infrared, “causality-limited” gravitational wave spectrum from causal processes in general cosmologies; we now briefly review this formalism, concentrating on modes that were outside the horizon during the phase transition.⁷ We focus on the effect of free-streaming radiation studied in Ref. [88] and then extend results to interacting scenarios as studied in the previous section.

4.1 Results in noninteracting scenarios

On scales sufficiently larger than those that are dynamical during the phase transition, the anisotropic stress tensor (in Fourier space) is independent of wavenumber k [88, 187]. Furthermore, for gravitational waves with such long characteristic timescales, the phase transition essentially occurs instantaneously. Such superhorizon tensor modes are well described by an initial condition wherein the gravitational wave is spontaneously “kicked” at the time τ_i of the phase transition:

$$h_\lambda(\tau_i, \mathbf{k}) = 0 \quad (4.1a)$$

$$\partial_\tau h_\lambda(\tau_i, \mathbf{k}) = J_i \quad (4.1b)$$

$$F_{\lambda,l}^{(T)}(\tau_i, \mathbf{k}) = 0. \quad (4.1c)$$

In general, the wavenumber-independent magnitude of the source J_i depends on the details of the subhorizon source. While these initial conditions (and the equations themselves, in a radiation Universe) are independent of wavenumber, the resulting solutions are not: each mode spends a different amount of time outside the horizon after being sourced. As a result, the low-frequency tail of the gravitational wave spectrum can carry information about the equation of state and free-streaming content of the Universe (and the time dependence thereof) during this period. Ref. [88] showed that, in terms of the equation of state of the Universe w and in the absence of free-streaming particles, the spectrum (for wavenumbers that were superhorizon during the phase transition) scales as

$$\Omega_{\text{GW}}(\tau, k) \propto k^{(1+15w)/(1+3w)}, \quad (4.2)$$

reproducing the well-known k^3 behavior in a radiation Universe.

The superhorizon modes in this case are (strongly) overdamped, sourced harmonic oscillators. Soon after being sourced, the gravitational wave approaches a constant-amplitude solution with $h_\lambda \approx J_i/\mathcal{H}(\tau_i)$ if its wavenumber is sufficiently smaller than the horizon ($k\tau_i \lesssim 10^{-3/2}$)—otherwise, it begins oscillating before saturating this maximal, frozen amplitude. After this point they resemble inflationary gravitational waves, suggesting that the damping effect of free-streaming radiation at horizon crossing is still relevant. However, their initial velocity also sources anisotropic stress in free-streaming particles [evident in the formal solution for $F_\lambda^{(T)}$, Eq. (2.38)]. As shown by Ref. [88], the damping effect of free-streaming particles is more important just after h_λ is “kicked” than after horizon crossing, leading to a qualitatively different signature. To understand the resulting dynamics outside the horizon, take the $k\tau \ll 1$ limit of the integral equation, Eq. (2.39). As $K(y) = 1/15 + \mathcal{O}(y^2)$, the gravitational wave then evolves according to⁸

$$\partial_x^2 h_\lambda + 2 \frac{\partial_x a}{a} \partial_x h_\lambda + h_\lambda = -\frac{8}{5} f_{\text{is}} \left(\frac{\partial_x a}{a} \right)^2 [h_\lambda(x) - h_\lambda(x_i)]. \quad (4.3)$$

⁷Though the treatment is agnostic to the nature of the subhorizon physics at play, we follow Ref. [88] in simply referring to it as a phase transition.

⁸This limit is applicable to inflationary gravitational waves as discussed in Section 3.2 but is irrelevant: frozen-out gravitational waves have negligible velocity, so the right-hand side of Eq. (4.3) is likewise small when well outside the horizon.

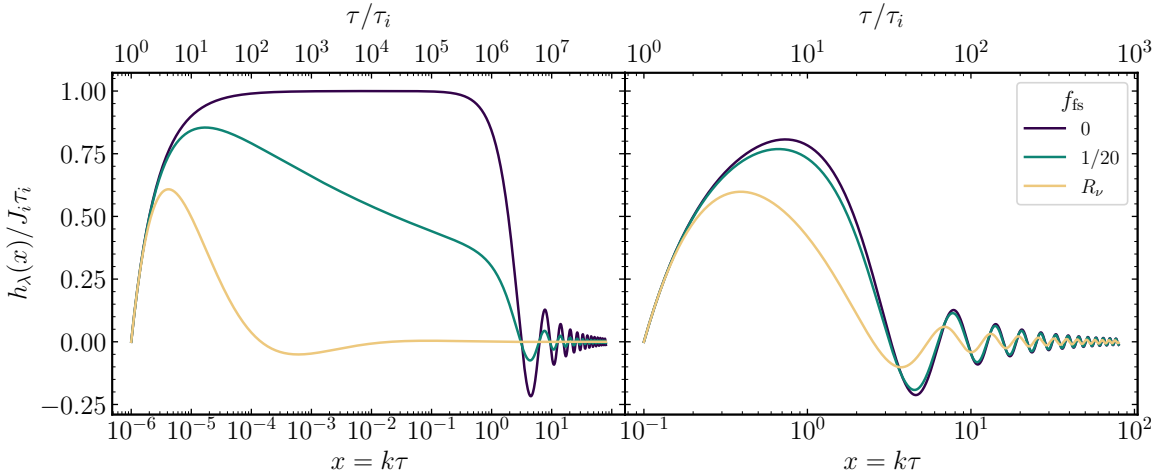


Figure 5. Dynamics of causal gravitational waves (in a radiation Universe) with wavelengths 10^6 (left panel) and 10 (right panel) times larger than the horizon at the time of the phase transition, τ_i . Each curve fixes a different abundance of free-streaming radiation f_{fs} as labeled in the legend. Note that the bottom axes are in units of $1/k$, i.e., the time of horizon crossing, while the top ones are in units of τ_i , the time of the phase transition. Results are normalized by $J_i/\mathcal{H}(\tau_i) = J_i\tau_i$, the maximal amplitude that sufficiently superhorizon modes freeze out to.

In radiation domination [Eq. (2.21)] with f_{fs} constant, the solution to Eq. (4.3) from the causal initial condition Eq. (4.1) is given in terms of spherical Bessel functions as

$$h_\lambda(x) = \frac{J_i x_i^2}{k} [j_\gamma(x_i) y_\gamma(x) - j_\gamma(x) y_\gamma(x_i)], \quad (4.4)$$

where

$$\gamma = \frac{-1 + \sqrt{1 - 32f_{\text{fs}}/5}}{2}. \quad (4.5)$$

Equation (4.4) provides a decent approximation to full numerical solutions, the latter of which we display in Fig. 5. By $\tau \sim 5\tau_i$, free-streaming radiation reduces the gravitational wave amplitude first attained after the kick—by as much as a factor of two for $f_{\text{fs}} = 1$. After this point, the dynamics are qualitatively dependent on the abundance of free-streaming radiation. When the Universe comprises entirely fluidlike radiation ($f_{\text{fs}} = 0$), modes with sufficiently small wavenumber k freeze as discussed above, after which point they behave like inflationary gravitational waves. On the other hand, if $k\tau_i \gtrsim 10^{-1}$, as in the right-hand panel of Fig. 5, modes reenter the horizon before fully freezing, i.e., have nonzero amplitude and velocity when they begin to oscillate.

In stark contrast, in the presence of free-streaming radiation gravitational waves evolve while outside the horizon. To understand the dynamics in Fig. 5, observe that in the superhorizon limit of the equation of motion [Eq. (4.3)] free-streaming particles appear to induce a mass for gravitational waves proportional to the Hubble scale. Indeed, after jumping up to its maximal amplitude, the tensor perturbation slowly rolls in this effective potential. The superhorizon damping is therefore stronger on larger scales, as the tensor perturbation rolls more toward zero the longer it remains outside the horizon (evident in comparing the two panels of Fig. 5). For small free-streaming fractions $f_{\text{fs}} \lesssim 10^{-1}$ (and so small effective masses), the effect is monotonic, but for larger values the gravitational wave can in fact cross zero while still outside the horizon. For $f_{\text{fs}} \gtrsim 1/2$, it completes one highly damped oscillation while outside the horizon before decaying toward increasingly small values. These results

are summarized by the empirical results [88, 89]

$$\frac{\Omega_{\text{GW}}}{\Omega_{\text{GW}}[f_{\text{fs}} = 0]} \approx \begin{cases} (k\tau_i)^{16f_{\text{fs}}/5} & f_{\text{fs}} \lesssim 5/32 \\ k\tau_i \left(C_1 + C_2 \sin \left[\sqrt{32f_{\text{fs}}/5} \ln(k\tau_i) + C_3 \right] \right) & f_{\text{fs}} \gtrsim 5/32 \end{cases} \quad (4.6)$$

where the C_a are mildly f_{fs} -dependent factors.

4.2 Results in interacting scenarios

We now turn to the effect of decoupling or recoupling self-interactions. Since the superhorizon dynamics are well described by a simple ordinary differential equation [Eq. (4.3)], analytic results for instantaneous transitions could feasibly be obtained by matching solutions between the interacting and noninteracting regimes. We instead simply discuss numerical results for self-interactions mediated by heavy ($n = 5$) and light ($n = 1$) mediators as considered previously.

The suppression of causal gravitational waves depends on the precise timing of de-/recoupling relative to the time of the phase transition, when the mode would reach its superhorizon, frozen amplitude, and when it reenters the horizon. The results are therefore complex and at times can be moderately sensitive to the precise timing of de-/recoupling relative to one of the other relevant timescales. We now summarize the relevant regimes and present results for a set of representative scenarios, focusing on the effect of the timing of de-/recoupling relative to the time of the phase transition, τ_*/τ_i . Figure 6 displays the squared damping factor for all scenarios considered, each of which we discuss in turn. Note that the quantity plotted in Fig. 6 multiplies the spectrum in Eq. (4.2), i.e., acts as a scale-dependent suppression on top of the standard k^3 dependence of Ω_{GW} for modes that were superhorizon during the phase transition (assuming a radiation-dominated Universe).

We first consider the decoupling of interactions, depicted in the left panels of Fig. 6. We consider two concrete scenarios: one where the relativistic species contains $\Omega_\nu = 1/20$ th of the energy density in the Universe and another with $\Omega_\nu = 0.40523$, as would be relevant for, e.g., dark phase transitions occurring around the time neutrinos decouple from the weak interactions. These would respectively belong to the small- and large- f_{fs} regimes of Eq. (4.6). Naturally, if decoupling occurs before the phase transition ($\tau_* < \tau_i$), the results match the noninteracting scenario, as evident in Fig. 6 where the darkest purple curves (with smallest τ_*/τ_i) resemble the dotted grey (depicting the fully noninteracting case). The noninteracting result is not precisely reproduced for τ_* slightly smaller than τ_i merely because decoupling is not instantaneous (for the T^5 interaction rate employed).

The next-simplest regime is that which behaves in exact analogy to inflationary gravitational waves: if $\tau_* \gtrsim 10^{3/2}\tau_i$, then all superhorizon modes reach the constant-amplitude solution before decoupling. The onset of free streaming at τ_* has no immediate effect because the gravitational wave’s velocity is too small to source anisotropic stress, but indeed damps any modes that subsequently enter the horizon (apparent in the green through yellow curves in Fig. 6).

When decoupling occurs sooner after the phase transition ($\tau_i < \tau_* \lesssim 10^{3/2}\tau_i$), the results are more complex. Efficient interactions suppress the neutrinos’ response to the “kick” (i.e., the nonzero gravitational-wave velocity), and, once they decouple, anisotropic stress can be sourced and damp gravitational waves. Because the gravitational wave is strongly damped after being kicked, its velocity is reduced at the time of decoupling and thus sources less anisotropic stress. For $\Omega_\nu = 1/20$, Fig. 6 makes apparent that the net effect is a reduced tilt in the damping effect, mimicking the effect of a parametrically smaller value of f_{fs} with no other scale-dependent features. The results are substantially more complex for larger Ω_ν (as in the bottom-left panel of Fig. 6) because of the oscillatory superhorizon dynamics. Intriguingly, if decoupling occurs near the time of the phase transition ($\tau_* \approx \tau_i$), a prominent dip appears in the spectrum in the range $10^{-3} \lesssim k\tau_i \lesssim 10^{-2}$. The solutions are difficult to describe in this case, as modes in this range reenter the horizon with varying amplitude and velocity.

We now turn to the recoupling scenarios depicted in the right panels of Fig. 6, considering the same values of Ω_ν . For recoupling occurring just before the phase transition ($\tau_* \lesssim \tau_i$), a small and nearly scale-independent amplitude suppression occurs because interactions do not become efficient instantaneously. For later recoupling, the effective mass vanishes simultaneously for all modes that are still superhorizon. As a result, the damping factor is scale independent for wavenumbers outside the

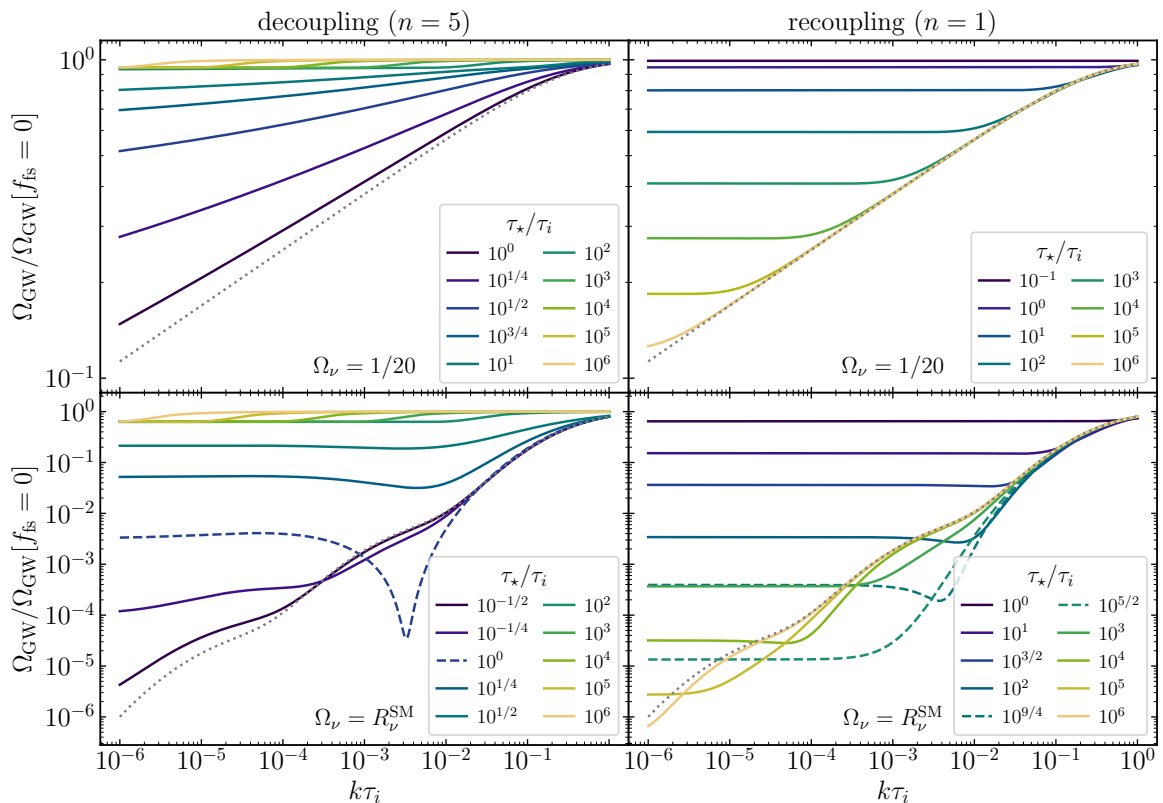


Figure 6. Damping factor for causal gravitational waves in scenarios with interacting radiation. The left and right panels respectively depict decoupling ($n = 5$) and recoupling ($n = 1$) scenarios. The top panels set the abundance of the relativistic species to $\Omega_\nu = 1/20$, while the bottom take $\Omega_\nu = R_\nu^{\text{SM}}$, i.e., that of neutrinos after electron-positron annihilation [Eq. (2.23)]. Each panel plots results for a set of de-/recoupling times relative to the phase transition (τ_\star/τ_i) with colors labeled by each legend as well as that for the fully noninteracting case (dotted grey). Some curves in the bottom panels are dashed to aid in distinguishing their unique behavior. The damping factor is normalized to the result for a scenario without free-streaming particles and plotted as a function of wavenumber k in units of the horizon size at the phase transition, $1/\tau_i$.

horizon at recoupling, leading to a broken power law in the regime of small free-streaming fraction as evident in the top-right panel of Fig. 6.

In the large- Ω_ν regime, the amplitude suppression still interpolates between that of the noninteracting scenario (for $k \gg k_\star$) and a constant suppression (for $k \ll k_\star$), but the intermediate regime can be more complex. In particular, for $\tau_\star \gtrsim 10\tau_i$ recoupling occurs while superhorizon modes are oscillating due to the induced effective mass, at which point they freeze out. The precise timing of these oscillations and recoupling again leads to a nontrivial spectral shape: modes with $k \sim k_\star$ may end up more damped than if interactions had persisted (thereby allowing them to continue to evolve outside the horizon). For example, when $\tau_\star = 10^{9/4}\tau_i$ the damping factor exhibits a modest dip near the horizon scale at recoupling. For $\tau_\star = 10^{10/4}\tau_i$, recoupling occurs when all modes still outside the horizon are at a point in their superhorizon oscillation of especially low amplitude. After recoupling these modes freeze at that amplitude, incurring a net damping one to two orders of magnitude greater than that if recoupling had occurred slightly earlier or later. In sum, the interplay of recoupling and the unique superhorizon evolution of causal gravitational waves coupled to free-streaming radiation permits conspicuous features in the (otherwise near-power-law) spectrum at low frequencies, without requiring any particular tuning of the times of recoupling and the phase transition.

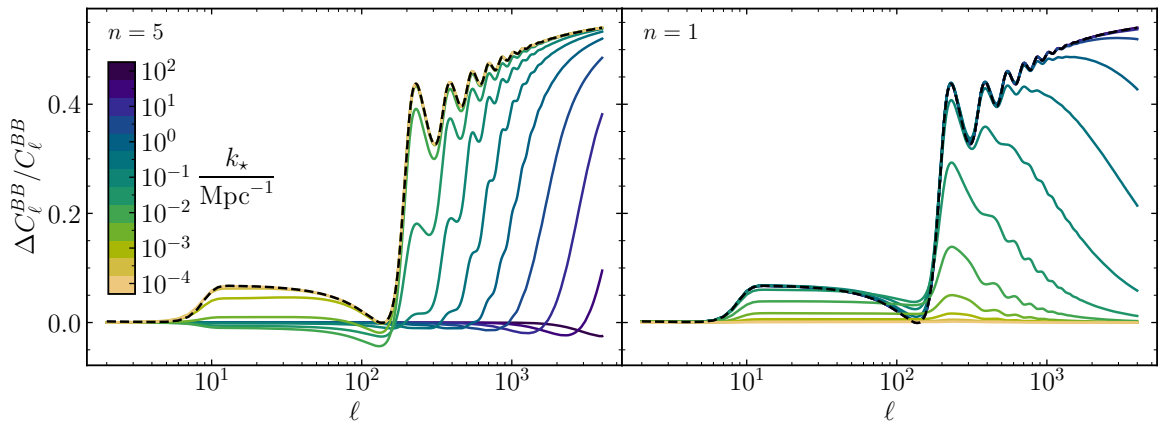


Figure 7. Relative change in the B -mode spectrum (compared to the SM case) in scenarios where nonstandard neutrino self-interactions decouple ($n = 5$, left) and recouple ($n = 1$, right). The colored curves vary the horizon size at de-/recoupling k_* from 10^{-4} Mpc^{-1} to 10^2 Mpc^{-1} as indicated by the colorbar. The dashed black curves display the limiting case of a Universe without neutrinos (but with the radiation density unchanged).

5 Discussion

In this paper we investigated the gravitational-wave signatures of the interaction history of relativistic particles. If a nonnegligible fraction of the Universe’s energy budget resides in radiation with self-interactions (whether the Standard Model neutrinos or species from dark sectors), the transition between strongly and weakly interacting regimes imprints characteristic features in primordial gravitational wave backgrounds. For gravitational waves seeded during inflation, the effect takes the form of a sigmoidal modulation in amplitude, since the anisotropic stress generated by collisionless or free-streaming particles damps gravitational waves as modes reenter the horizon. On the other hand, if subhorizon dynamics (such as a first-order phase transition) source a substantial gravitational wave background in the early Universe, superhorizon gravitational waves (at frequencies well below the peak of the signal) are also generated and respond to the presence of free-streaming particles even before horizon crossing. Both of these scenarios permit model-agnostic descriptions of gravitational waves seeded outside the cosmological horizon. Because the coupling of gravitational waves to relativistic particles decays inside the horizon, these two cases combine to provide a nearly comprehensive treatment of the imprint of the decoupling or recoupling of interactions.⁹

We now consider possible avenues for observing the signature of decoupling or recoupling interactions in the gravitational wave background. The primordial background from inflation, though well motivated, has yet eluded observation. In the near term, the most promising means to detect inflationary gravitational waves is via the B -mode polarization of the CMB, which would be sensitive to neutrino self-interactions that become (in)efficient when observable modes enter the horizon. In Fig. 7 we display the relative change in the B -mode angular power spectrum for representative decoupling and recoupling scenarios, computed by modifying CLASS [192] to include the interactions described in Section 2.2. Compared to the SM result, B -mode power is enhanced by as much as $\sim 50\%$ at small scales if neutrinos are fluidlike at early times. (The effect would be proportionally smaller if only one or two neutrino flavors interact, as in Fig. 4, or if considering radiation from a dark sector.) The same transition in amplitude observed in the gravitational wave power spectrum (Fig. 3) is evident

⁹One source of near-horizon-sized gravitational waves not captured by the inflationary or causal descriptions is the anisotropic stress induced by scalar metric perturbations at second order in perturbation theory [188–190]. Refs. [189, 191] computed the signal on large scales sourced by the standard adiabatic perturbations, accounting for photon and neutrino anisotropic stress. The possibility of primordial black hole dark matter has motivated much interest in gravitational waves induced by enhanced density fluctuations on small scales (see Ref. [190] and reference therein); the effect of anisotropic stress—which affects scalar perturbations at first order as well—would likely be difficult to account for in a model-independent manner.

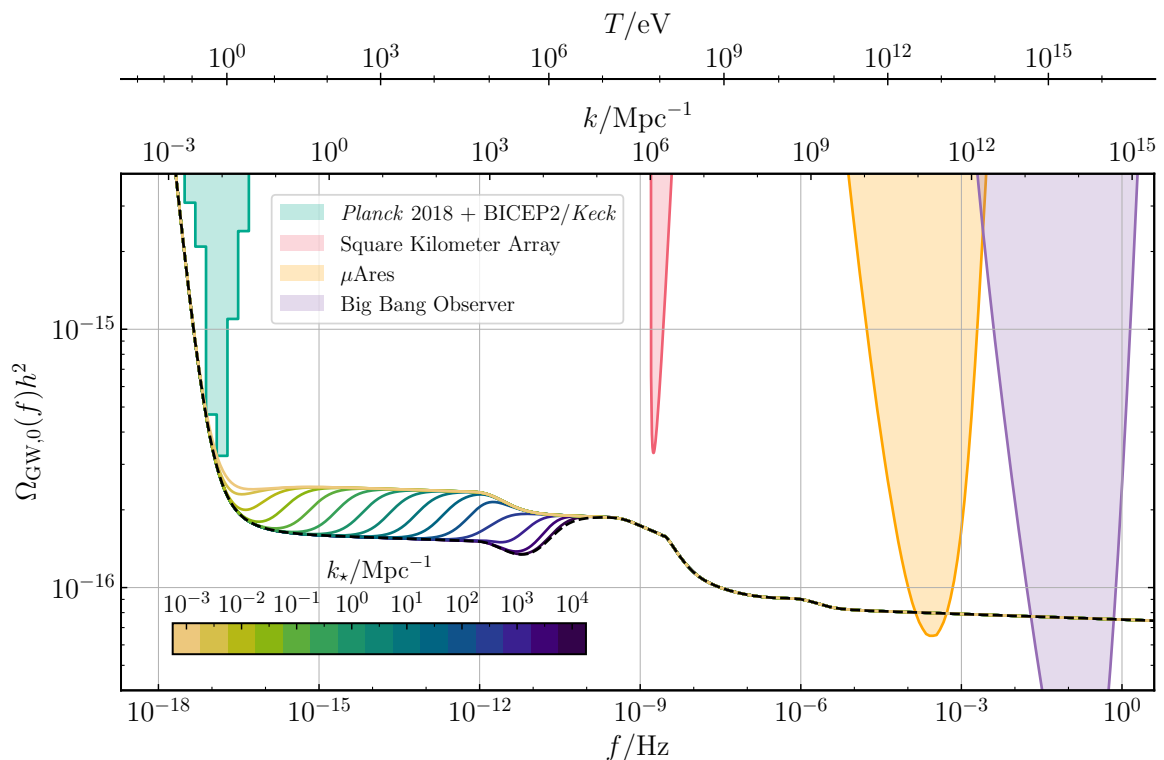


Figure 8. Spectral energy density in inflationary gravitational waves in decoupling scenarios that delay neutrino free streaming relative to the decoupling of the weak interactions. Colored curves display results for scenarios with interaction rate proportional to T^5 and various strengths parameterized in terms of the horizon size at decoupling (indicated by the colorbar), while the black dashed curve corresponds to the Standard Model result. All results assume single-field slow roll inflation with $r = 0.056$ and account for thermal history effects in Eq. (2.8) using data from Ref. [68]. Superimposed are recent constraints from *Planck* and BICEP2/Keck [12, 198] as computed by Ref. [106], forecasted power-law-integrated sensitivities of the Square Kilometre Array [58–60] and the proposed Big-Bang Observer [52–54], both, provided by Refs. [199, 200], and that of the proposed μAres detector [201], with color labeled by the legend.

over a finite range of multipoles, a steplike feature that would measure the horizon size at the time of decoupling or recoupling. These results generalize those of Ref. [141] (at a phenomenological level), which considered two specific models of neutrino–dark-matter interactions.

In addition, if interactions are important at sufficiently late times, a phase offset in the tensor modes’ temporal evolution (due to the presence or absence of anisotropic stress) shifts the analog of the acoustic peaks in the temperature and E -mode polarization spectra. More generally, the locations of the peaks in the primordial B -mode spectrum in principle provide a measure of the abundance of free-streaming vs. fluidlike radiation just as the acoustic peaks do [75]. Such features could help disentangle the effects of neutrino interactions from the amplitude and tilt of the primordial tensor power spectrum. Furthermore, given the current mild discord between *Planck* and ACT in searches for evidence of strongly interacting neutrinos [85, 163] and early dark energy [193–196], information from tensor perturbations (which depend on comparatively simpler physics than scalars) could provide a crucial independent probe.

Further in the future, pulsar timing and interferometers will provide a high-frequency lever arm for measuring an inflationary gravitational wave background, jointly limiting the amplitude and tilt of the inflationary spectrum [50]. Measurements at disparate scales would also probe the abundance of free-streaming radiation over a large span of temperatures [149, 197], a possibility we consider in Fig. 8. Though the dearth of proposed methods for observing gravitational waves near picohertz

frequencies is unfortunate for the prospects of probing neutrino decoupling, observations at higher frequencies—whether of inflationary or causal gravitational waves—would probe new particles that decouple from the SM plasma while relativistic. Current constraints limit such light relics to comprise $\lesssim 4\%$ of the radiation budget at the time of the CMB, but their relative contribution would be roughly twice as large at temperatures above the electroweak scale [202]. Larger abundances of free-streaming radiation in the very early Universe can be accommodated by more exotic cosmologies (if, say, that radiation later decays, or other degrees of freedom inject entropy into the SM plasma).

In more speculative scenarios, the low-frequency gravitational wave signal from causal, subhorizon processes, such as phase transitions or resonant particle production, would be sensitive to the interaction history of radiation. The low-frequency tail (i.e., modes that were superhorizon at the time of production) is tilted blue (relative to the typical f^3 dependence) under the influence of tensor anisotropic stress; the decoupling or recoupling of interactions in relativistic species would lead to a break in the power law, evident in Fig. 6. If the abundance of free-streaming radiation is large ($f_{\text{fs}} \gtrsim 5/32$), additional oscillatory features arise. Ref. [89] demonstrated that future space-borne interferometers could optimistically probe, through measurements of the causal tail from phase transitions, the thermal history of the Universe at the percent or permille level—including the effect of a single new light, free-streaming particle. The effects of decoupling or recoupling observed in Fig. 6 could likely be probed to the same degree. Finally, dark sector dynamics that source gravitational waves after neutrino decoupling but before recombination (as motivated by, e.g., early dark energy [41, 203, 204] and the axiverse [38, 205]) could produce signals visible to future CMB experiments that would be sensitive to whether neutrinos interact or free-stream. The discovery of gravitational wave backgrounds from such novel scenarios (or from inflation or phase transitions) would provide an exciting opportunity to learn about not just the physics underlying their sources but also possible nonstandard neutrino interactions, dark radiation sectors, and the dynamics of the early Universe over a broad range of energy scales.

Acknowledgments

This research is supported by the Department of Physics and the College of Arts and Sciences at the University of Washington. ML is grateful for support from the Dr. Ann Nelson Endowed Professorship in Physics. This work made use of the Python packages NumPy [206], SciPy [207], matplotlib [208], SymPy [209], mpmath [210], and CMasher [211].

A Numerical implementation

In this appendix we outline the numerical implementation of the various calculations performed in this work. Regardless of the background evolution (for radiation and matter-radiation Universes) or of the initial conditions (inflationary or causal), we solve Eq. (2.20) with the Boltzmann hierarchy for $F^{(T)}$ truncated at $l_{\text{max}} = 100$ with the truncation prescription of Ref. [107],

$$F_{\lambda, l_{\text{max}}} \approx \frac{2l_{\text{max}} - 1}{k\tau} F_{\lambda, l_{\text{max}}-1} - F_{\lambda, l_{\text{max}}-2}. \quad (\text{A.1})$$

We use SciPy’s [207] `solve_ivp` routine to solve the system numerically. For noninteracting scenarios, we use the explicit Runge-Kutta method DOP853 [212] with relative tolerance 10^{-6} and absolute tolerance 10^{-12} . The self-interaction terms, on the other hand, make the system stiff and better suited to implicit methods; in this case we use the Radau IIA routine [213] with the Jacobian of Eq. (2.20) computed by hand (i.e., analytically) as a sparse matrix. To reduce the sensitivity of the adaptive time stepping to the exponentially damped $F_{\lambda, l}$ (whenever interactions are efficient), we increase its absolute tolerance to 10^{-9} and decrease that of h_λ and $\partial_x h_\lambda$ to 10^{-15} .

In all cases, we evolve the system to $x_f \equiv k\tau_f = 100$; the chosen $l_{\text{max}} = 100$ safely ensures that errors from the truncation of the Boltzmann hierarchy do not propagate back to the first few moments until $k\tau \sim 100$ (at which point the anisotropic stress itself is small anyway). To compute the damping coefficient A_∞ , we match on to the solution to Eq. (2.20b) in a Universe with constant equation of

state and no anisotropic stress,

$$h_\lambda(x) = \frac{x_f^{\alpha+1}}{x^{\alpha-1}} (-j_{\alpha-1}(x) [y_\alpha(x_f) h_\lambda(x_f) + y_{\alpha-1}(x_f) h'_\lambda(x_f)] + y_{\alpha-1}(x) [j_\alpha(x_f) h_\lambda(x_f) + j_{\alpha-1}(x_f) h'_\lambda(x_f)]). \quad (\text{A.2})$$

Here primes denote derivatives with respect to x . When both x and x_f are large,

$$A_\infty \approx a(x_f/k) \sqrt{h_\lambda(x_f)^2 + h'_\lambda(x_f)^2}. \quad (\text{A.3})$$

In a single component Universe, $a(x_f/k) = x_f^\alpha$ (normalized to the scale factor at horizon crossing) and Eq. (A.3) holds asymptotically (and at all times in radiation Universes). These results are also accurate in matter-radiation Universes if evaluated when modes are deep inside the horizon, since the Hubble rate then changes slowly compared to the gravitational-wave oscillation frequency. We have verified that these approximations achieve subpercent accuracy in evaluating the relative effect of neutrinos compared to Universes with only fluidlike radiation. See, e.g., Refs. [108, 186, 214] for more formal procedures to match analytic solutions between the radiation and matter eras.

To compute the B -mode power spectrum of the CMB, we modify CLASS to include neutrino interactions in the same manner. (CLASS of course implements a complete Λ CDM cosmology that accounts for dark energy at late times.) CLASS's implicit solver is less robust to the equations becoming extremely stiff (e.g., at very early times for decoupling scenarios), so we cap the maximum value of the interaction rate to 10^{12} Mpc^{-1} and verified that increasing or decreasing this value had a negligible impact on the results.

B Semianalytic results for inflationary gravitational waves

This appendix outlines the computation that yields the semianalytic results for the amplitude and phase of inflationary gravitational waves in the presence of free-streaming particles, Eqs. (3.2a) and (3.2b).

Following Ref. [178–180], express the convolution of spherical Bessel functions as a series thereof:

$$-\int_0^x du K(x-u) \partial_u j_0(u) = \sum_{n=0}^{\infty} c_n j_n(x). \quad (\text{B.1})$$

[Recall that $\partial_u j_0(u) = -j_1(u)$.] Eq. (24) of Ref. [179] provides an analytic result for the convolution in Eq. (B.1) in terms of Clebsch-Gordan coefficients, which we evaluate using SymPy [209]. Only the even c_n are nonzero, due to symmetry properties of the Clebsch-Gordan coefficients (see Refs. [178–180] for details).

In order to compute the amplitude and phase [Eqs. (3.2a) and (3.2b)], we must obtain \mathcal{I}_s and \mathcal{I}_c from Eq. (2.49), which in turn requires integrating the order-zero spherical Bessel functions against spherical Bessel functions. In terms of the hypergeometric function ${}_2F_3$, these evaluate to

$$\int_0^x d\tilde{x} j_n(\tilde{x}) y_0(\tilde{x}) = -\frac{\sqrt{\pi} x^n}{2^{n+1} n \Gamma(n+3/2)} {}_2F_3 \left(\frac{n+1}{2}, \frac{n}{2}; \frac{1}{2}, n+1, n+\frac{3}{2}; -x^2 \right) \quad (\text{B.2a})$$

$$\int_0^x d\tilde{x} j_n(\tilde{x}) j_0(\tilde{x}) = \frac{\pi x^{n+1}}{2^{n+2} \Gamma(3/2) \Gamma(n+3/2) \Gamma(n+2)} {}_2F_3 \left(\frac{n+1}{2}, \frac{n}{2}+1; \frac{3}{2}, \frac{3}{2}+n, n+2; -x^2 \right). \quad (\text{B.2b})$$

For even $n > 0$, the series expansions of the above about large x are

$$\int_0^x d\tilde{x} j_n(\tilde{x}) y_0(\tilde{x}) = -\frac{(-1)^{n/2}}{n(n+1)} + \frac{1}{x^2} \frac{(-1)^{n/2}}{8} [n(n+1) + 2 \cos(2x)] + \mathcal{O}(x^{-3}) \quad (\text{B.3a})$$

$$\int_0^x d\tilde{x} j_n(\tilde{x}) j_0(\tilde{x}) = -\frac{(-1)^{n/2}}{2x} \left[1 + \frac{\cos x \sin x}{x} \right] + \mathcal{O}(x^{-3}). \quad (\text{B.3b})$$

We observe that $|c_n| \sim n^{-5}$ for large n , so the series appearing in \mathcal{I}_s and \mathcal{I}_c [i.e., after substituting Eq. (B.3) into Eq. (2.49)] converge. Numerically evaluating the required series (up to 256 – 512 terms) yields

$$24 \sum_{m=1}^{\infty} (-1)^m c_{2m} \approx -2 \quad (\text{B.4a})$$

$$24 \sum_{m=1}^{\infty} \frac{(-1)^m}{2m(2m+1)} c_{2m} \approx -\frac{5}{9} \quad (\text{B.4b})$$

$$24 \sum_{m=1}^{\infty} (-1)^m \cdot 2m(2m+1) c_{2m} \approx 4. \quad (\text{B.4c})$$

Therefore, to leading order in large x , Eq. (2.49) evaluates to

$$\mathcal{I}_s(x) \approx -h_{\lambda,0} f_{\text{fs}} \left(\frac{5}{9} + \frac{1}{x^2} \sin^2 x \right) \quad (\text{B.5a})$$

$$\mathcal{I}_c(x) \approx -h_{\lambda,0} \frac{f_{\text{fs}}}{x} \left(1 + \frac{\cos x \sin x}{x} \right). \quad (\text{B.5b})$$

Substituting these asymptotic expansions into Eqs. (2.51) and (2.52) yields Eqs. (3.2a) and (3.2b).

References

- [1] CMB-S4 collaboration, *Snowmass 2021 CMB-S4 White Paper*, in *2022 Snowmass Summer Study*, 3, 2022 [[2203.08024](#)].
- [2] C.L. Chang et al., *Snowmass2021 Cosmic Frontier: Cosmic Microwave Background Measurements White Paper*, [2203.07638](#).
- [3] CMB-S4 collaboration, *CMB-S4 Science Book, First Edition*, [1610.02743](#).
- [4] CMB-S4 collaboration, *CMB-S4: Forecasting Constraints on Primordial Gravitational Waves*, *Astrophys. J.* **926** (2022) 54 [[2008.12619](#)].
- [5] SPT-3G collaboration, *SPT-3G: A Next-Generation Cosmic Microwave Background Polarization Experiment on the South Pole Telescope*, *Proc. SPIE Int. Soc. Opt. Eng.* **9153** (2014) 91531P [[1407.2973](#)].
- [6] M. Kamionkowski and E.D. Kovetz, *The Quest for B Modes from Inflationary Gravitational Waves*, *Ann. Rev. Astron. Astrophys.* **54** (2016) 227 [[1510.06042](#)].
- [7] S. Staggs, J. Dunkley and L. Page, *Recent discoveries from the cosmic microwave background: a review of recent progress*, *Rept. Prog. Phys.* **81** (2018) 044901.
- [8] SIMONS OBSERVATORY collaboration, *The Simons Observatory: Science goals and forecasts*, *JCAP* **02** (2019) 056 [[1808.07445](#)].
- [9] C. Caprini and D.G. Figueroa, *Cosmological Backgrounds of Gravitational Waves*, *Class. Quant. Grav.* **35** (2018) 163001 [[1801.04268](#)].
- [10] BICEP, KECK collaboration, *Improved Constraints on Primordial Gravitational Waves using Planck, WMAP, and BICEP/Keck Observations through the 2018 Observing Season*, *Phys. Rev. Lett.* **127** (2021) 151301 [[2110.00483](#)].
- [11] E. Komatsu, *New physics from the polarised light of the cosmic microwave background*, [2202.13919](#).
- [12] PLANCK collaboration, *Planck 2018 results. X. Constraints on inflation*, *Astron. Astrophys.* **641** (2020) A10 [[1807.06211](#)].
- [13] PLANCK collaboration, *Planck 2018 results. VI. Cosmological parameters*, *Astron. Astrophys.* **641** (2020) A6 [[1807.06209](#)].

- [14] A.A. Starobinsky, *Spectrum of relict gravitational radiation and the early state of the universe*, *JETP Lett.* **30** (1979) 682.
- [15] A.H. Guth, *The Inflationary Universe: A Possible Solution to the Horizon and Flatness Problems*, *Phys. Rev. D* **23** (1981) 347.
- [16] K. Sato, *First Order Phase Transition of a Vacuum and Expansion of the Universe*, *Mon. Not. Roy. Astron. Soc.* **195** (1981) 467.
- [17] V.F. Mukhanov and G.V. Chibisov, *Quantum Fluctuations and a Nonsingular Universe*, *JETP Lett.* **33** (1981) 532.
- [18] A.D. Linde, *A New Inflationary Universe Scenario: A Possible Solution of the Horizon, Flatness, Homogeneity, Isotropy and Primordial Monopole Problems*, *Phys. Lett. B* **108** (1982) 389.
- [19] A. Albrecht and P.J. Steinhardt, *Cosmology for Grand Unified Theories with Radiatively Induced Symmetry Breaking*, *Phys. Rev. Lett.* **48** (1982) 1220.
- [20] A.D. Linde, *Chaotic Inflation*, *Phys. Lett. B* **129** (1983) 177.
- [21] A. Achúcarro et al., *Inflation: Theory and Observations*, [2203.08128](#).
- [22] LIGO SCIENTIFIC, VIRGO collaboration, *Observation of Gravitational Waves from a Binary Black Hole Merger*, *Phys. Rev. Lett.* **116** (2016) 061102 [[1602.03837](#)].
- [23] NANOGrav collaboration, *The NANOGrav 12.5 yr Data Set: Search for an Isotropic Stochastic Gravitational-wave Background*, *Astrophys. J. Lett.* **905** (2020) L34 [[2009.04496](#)].
- [24] S.W. Ballmer et al., *Snowmass2021 Cosmic Frontier White Paper: Future Gravitational-Wave Detector Facilities*, in *2022 Snowmass Summer Study*, 3, 2022 [[2203.08228](#)].
- [25] A. Kosowsky, M.S. Turner and R. Watkins, *Gravitational radiation from colliding vacuum bubbles*, *Phys. Rev. D* **45** (1992) 4514.
- [26] A. Kosowsky, M.S. Turner and R. Watkins, *Gravitational waves from first order cosmological phase transitions*, *Phys. Rev. Lett.* **69** (1992) 2026.
- [27] M. Kamionkowski, A. Kosowsky and M.S. Turner, *Gravitational radiation from first order phase transitions*, *Phys. Rev. D* **49** (1994) 2837 [[astro-ph/9310044](#)].
- [28] C. Grojean and G. Servant, *Gravitational Waves from Phase Transitions at the Electroweak Scale and Beyond*, *Phys. Rev. D* **75** (2007) 043507 [[hep-ph/0607107](#)].
- [29] C. Caprini et al., *Science with the space-based interferometer eLISA. II: Gravitational waves from cosmological phase transitions*, *JCAP* **04** (2016) 001 [[1512.06239](#)].
- [30] C. Caprini et al., *Detecting gravitational waves from cosmological phase transitions with LISA: an update*, *JCAP* **03** (2020) 024 [[1910.13125](#)].
- [31] T.W.B. Kibble, *Topology of Cosmic Domains and Strings*, *J. Phys. A* **9** (1976) 1387.
- [32] A. Vilenkin, *Gravitational Field of Vacuum Domain Walls and Strings*, *Phys. Rev. D* **23** (1981) 852.
- [33] T. Vachaspati and A. Vilenkin, *Gravitational Radiation from Cosmic Strings*, *Phys. Rev. D* **31** (1985) 3052.
- [34] T. Damour and A. Vilenkin, *Gravitational radiation from cosmic (super)strings: Bursts, stochastic background, and observational windows*, *Phys. Rev. D* **71** (2005) 063510 [[hep-th/0410222](#)].
- [35] J.J. Blanco-Pillado, K.D. Olum and X. Siemens, *New limits on cosmic strings from gravitational wave observation*, *Phys. Lett. B* **778** (2018) 392 [[1709.02434](#)].
- [36] P. Auclair et al., *Probing the gravitational wave background from cosmic strings with LISA*, *JCAP* **04** (2020) 034 [[1909.00819](#)].
- [37] LIGO SCIENTIFIC, VIRGO, KAGRA collaboration, *Constraints on Cosmic Strings Using Data from the Third Advanced LIGO–Virgo Observing Run*, *Phys. Rev. Lett.* **126** (2021) 241102 [[2101.12248](#)].
- [38] N. Kitajima, J. Soda and Y. Urakawa, *Gravitational wave forest from string axiverse*, *JCAP* **10** (2018) 008 [[1807.07037](#)].

- [39] C.S. Machado, W. Ratzinger, P. Schwaller and B.A. Stefanek, *Audible Axions*, *JHEP* **01** (2019) 053 [[1811.01950](#)].
- [40] A. Arvanitaki, S. Dimopoulos, M. Galanis, L. Lehner, J.O. Thompson and K. Van Tilburg, *Large-misalignment mechanism for the formation of compact axion structures: Signatures from the QCD axion to fuzzy dark matter*, *Phys. Rev. D* **101** (2020) 083014 [[1909.11665](#)].
- [41] Z.J. Weiner, P. Adshead and J.T. Giblin, *Constraining early dark energy with gravitational waves before recombination*, *Phys. Rev. D* **103** (2021) L021301 [[2008.01732](#)].
- [42] Y. Cui and E.I. Sfakianakis, *Detectable Gravitational Wave Signals from Inflationary Preheating*, [2112.00762](#).
- [43] T. Nakamura, M. Sasaki, T. Tanaka and K.S. Thorne, *Gravitational waves from coalescing black hole MACHO binaries*, *Astrophys. J. Lett.* **487** (1997) L139 [[astro-ph/9708060](#)].
- [44] R. Saito and J. Yokoyama, *Gravitational wave background as a probe of the primordial black hole abundance*, *Phys. Rev. Lett.* **102** (2009) 161101 [[0812.4339](#)].
- [45] M. Sasaki, T. Suyama, T. Tanaka and S. Yokoyama, *Primordial Black Hole Scenario for the Gravitational-Wave Event GW150914*, *Phys. Rev. Lett.* **117** (2016) 061101 [[1603.08338](#)].
- [46] S. Bird, I. Cholis, J.B. Muñoz, Y. Ali-Haïmoud, M. Kamionkowski, E.D. Kovetz et al., *Did LIGO detect dark matter?*, *Phys. Rev. Lett.* **116** (2016) 201301 [[1603.00464](#)].
- [47] M. Sasaki, T. Suyama, T. Tanaka and S. Yokoyama, *Primordial black holes—perspectives in gravitational wave astronomy*, *Class. Quant. Grav.* **35** (2018) 063001 [[1801.05235](#)].
- [48] B. Carr, K. Kohri, Y. Sendouda and J. Yokoyama, *Constraints on primordial black holes*, *Rept. Prog. Phys.* **84** (2021) 116902 [[2002.12778](#)].
- [49] T.L. Smith, M. Kamionkowski and A. Cooray, *Direct detection of the inflationary gravitational wave background*, *Phys. Rev. D* **73** (2006) 023504 [[astro-ph/0506422](#)].
- [50] P.D. Lasky et al., *Gravitational-wave cosmology across 29 decades in frequency*, *Phys. Rev. X* **6** (2016) 011035 [[1511.05994](#)].
- [51] N. Seto, S. Kawamura and T. Nakamura, *Possibility of direct measurement of the acceleration of the universe using 0.1-Hz band laser interferometer gravitational wave antenna in space*, *Phys. Rev. Lett.* **87** (2001) 221103 [[astro-ph/0108011](#)].
- [52] J. Crowder and N.J. Cornish, *Beyond LISA: Exploring future gravitational wave missions*, *Phys. Rev. D* **72** (2005) 083005 [[gr-qc/0506015](#)].
- [53] V. Corbin and N.J. Cornish, *Detecting the cosmic gravitational wave background with the big bang observer*, *Class. Quant. Grav.* **23** (2006) 2435 [[gr-qc/0512039](#)].
- [54] G.M. Harry, P. Fritschel, D.A. Shaddock, W. Folkner and E.S. Phinney, *Laser interferometry for the big bang observer*, *Class. Quant. Grav.* **23** (2006) 4887.
- [55] S. Kawamura et al., *The Japanese space gravitational wave antenna DECIGO*, *Class. Quant. Grav.* **23** (2006) S125.
- [56] K. Yagi and N. Seto, *Detector configuration of DECIGO/BBO and identification of cosmological neutron-star binaries*, *Phys. Rev. D* **83** (2011) 044011 [[1101.3940](#)].
- [57] S. Isoyama, H. Nakano and T. Nakamura, *Multiband Gravitational-Wave Astronomy: Observing binary inspirals with a decihertz detector, B-DECIGO*, *PTEP* **2018** (2018) 073E01 [[1802.06977](#)].
- [58] C.L. Carilli and S. Rawlings, *Science with the Square Kilometer Array: Motivation, key science projects, standards and assumptions*, *New Astron. Rev.* **48** (2004) 979 [[astro-ph/0409274](#)].
- [59] G. Janssen et al., *Gravitational wave astronomy with the SKA*, *PoS AASKA14* (2015) 037 [[1501.00127](#)].
- [60] A. Weltman et al., *Fundamental physics with the Square Kilometre Array*, *Publ. Astron. Soc. Austral.* **37** (2020) e002 [[1810.02680](#)].
- [61] M. Maggiore, *Gravitational wave experiments and early universe cosmology*, *Phys. Rept.* **331** (2000) 283 [[gr-qc/9909001](#)].

- [62] R. Caldwell et al., *Detection of Early-Universe Gravitational Wave Signatures and Fundamental Physics*, [2203.07972](#).
- [63] L.P. Grishchuk, *Amplification of gravitational waves in an isotropic universe*, *Zh. Eksp. Teor. Fiz.* **67** (1974) 825.
- [64] M. Giovannini, *Gravitational waves constraints on postinflationary phases stiffer than radiation*, *Phys. Rev. D* **58** (1998) 083504 [[hep-ph/9806329](#)].
- [65] L.A. Boyle and P.J. Steinhardt, *Probing the early universe with inflationary gravitational waves*, *Phys. Rev. D* **77** (2008) 063504 [[astro-ph/0512014](#)].
- [66] S. Kuroyanagi, K. Nakayama and S. Saito, *Prospects for determination of thermal history after inflation with future gravitational wave detectors*, *Phys. Rev. D* **84** (2011) 123513 [[1110.4169](#)].
- [67] B. Li, T. Rindler-Daller and P.R. Shapiro, *Cosmological Constraints on Bose-Einstein-Condensed Scalar Field Dark Matter*, *Phys. Rev. D* **89** (2014) 083536 [[1310.6061](#)].
- [68] K. Saikawa and S. Shirai, *Primordial gravitational waves, precisely: The role of thermodynamics in the Standard Model*, *JCAP* **05** (2018) 035 [[1803.01038](#)].
- [69] D.G. Figueroa and E.H. Tanin, *Ability of LIGO and LISA to probe the equation of state of the early Universe*, *JCAP* **08** (2019) 011 [[1905.11960](#)].
- [70] S. Weinberg, *Damping of tensor modes in cosmology*, *Phys. Rev. D* **69** (2004) 023503 [[astro-ph/0306304](#)].
- [71] P.F. de Salas, D.V. Forero, S. Gariazzo, P. Martínez-Miravé, O. Mena, C.A. Ternes et al., *2020 global reassessment of the neutrino oscillation picture*, *JHEP* **02** (2021) 071 [[2006.11237](#)].
- [72] I. Esteban, M.C. Gonzalez-Garcia, M. Maltoni, T. Schwetz and A. Zhou, *The fate of hints: updated global analysis of three-flavor neutrino oscillations*, *JHEP* **09** (2020) 178 [[2007.14792](#)].
- [73] S. Bashinsky and U. Seljak, *Neutrino perturbations in CMB anisotropy and matter clustering*, *Phys. Rev. D* **69** (2004) 083002 [[astro-ph/0310198](#)].
- [74] Z. Hou, R. Keisler, L. Knox, M. Millea and C. Reichardt, *How Massless Neutrinos Affect the Cosmic Microwave Background Damping Tail*, *Phys. Rev. D* **87** (2013) 083008 [[1104.2333](#)].
- [75] D. Baumann, D. Green, J. Meyers and B. Wallisch, *Phases of New Physics in the CMB*, *JCAP* **01** (2016) 007 [[1508.06342](#)].
- [76] G. Choi, C.-T. Chiang and M. LoVerde, *Probing Decoupling in Dark Sectors with the Cosmic Microwave Background*, *JCAP* **06** (2018) 044 [[1804.10180](#)].
- [77] B. Follin, L. Knox, M. Millea and Z. Pan, *First Detection of the Acoustic Oscillation Phase Shift Expected from the Cosmic Neutrino Background*, *Phys. Rev. Lett.* **115** (2015) 091301 [[1503.07863](#)].
- [78] N. Blinov and G. Marques-Tavares, *Interacting radiation after Planck and its implications for the Hubble Tension*, *JCAP* **09** (2020) 029 [[2003.08387](#)].
- [79] T. Brinckmann, J.H. Chang and M. LoVerde, *Self-interacting neutrinos, the Hubble parameter tension, and the cosmic microwave background*, *Phys. Rev. D* **104** (2021) 063523 [[2012.11830](#)].
- [80] F.-Y. Cyr-Racine and K. Sigurdson, *Limits on Neutrino-Neutrino Scattering in the Early Universe*, *Phys. Rev. D* **90** (2014) 123533 [[1306.1536](#)].
- [81] L. Lancaster, F.-Y. Cyr-Racine, L. Knox and Z. Pan, *A tale of two modes: Neutrino free-streaming in the early universe*, *JCAP* **07** (2017) 033 [[1704.06657](#)].
- [82] I.M. Oldengott, T. Tram, C. Rampf and Y.Y.Y. Wong, *Interacting neutrinos in cosmology: exact description and constraints*, *JCAP* **11** (2017) 027 [[1706.02123](#)].
- [83] G. Barenboim, P.B. Denton and I.M. Oldengott, *Constraints on inflation with an extended neutrino sector*, *Phys. Rev. D* **99** (2019) 083515 [[1903.02036](#)].
- [84] A. Das and S. Ghosh, *Flavor-specific interaction favors strong neutrino self-coupling in the early universe*, *JCAP* **07** (2021) 038 [[2011.12315](#)].
- [85] C.D. Kreisch et al., *The Atacama Cosmology Telescope: The Persistence of Neutrino Self-Interaction in Cosmological Measurements*, [2207.03164](#).

- [86] P. Taule, M. Escudero and M. Garny, *Global view of neutrino interactions in cosmology: The freestreaming window as seen by Planck*, [2207.04062](#).
- [87] S. Roy Choudhury, S. Hannestad and T. Tram, *Massive neutrino self-interactions and Inflation*, [2207.07142](#).
- [88] A. Hook, G. Marques-Tavares and D. Racco, *Causal gravitational waves as a probe of free streaming particles and the expansion of the Universe*, *JHEP* **02** (2021) 117 [[2010.03568](#)].
- [89] D. Brzemiński, A. Hook and G. Marques-Tavares, *Precision Early Universe Cosmology from Stochastic Gravitational Waves*, [2203.13842](#).
- [90] J.B. Dent, L.M. Krauss, S. Sabharwal and T. Vachaspati, *Damping of Primordial Gravitational Waves from Generalized Sources*, *Phys. Rev. D* **88** (2013) 084008 [[1307.7571](#)].
- [91] A. Ringwald, K. Saikawa and C. Tamarit, *Primordial gravitational waves in a minimal model of particle physics and cosmology*, *JCAP* **02** (2021) 046 [[2009.02050](#)].
- [92] G. Baym, S.P. Patil and C.J. Pethick, *Damping of gravitational waves by matter*, *Phys. Rev. D* **96** (2017) 084033 [[1707.05192](#)].
- [93] R. Flauger and S. Weinberg, *Gravitational Waves in Cold Dark Matter*, *Phys. Rev. D* **97** (2018) 123506 [[1801.00386](#)].
- [94] N. Mirón-Granese, *Relativistic viscous effects on the primordial gravitational waves spectrum*, *JCAP* **06** (2021) 008 [[2012.11422](#)].
- [95] M. Zarei, N. Bartolo, D. Bertacca, A. Ricciardone and S. Matarrese, *Non-Markovian open quantum system approach to the early Universe: Damping of gravitational waves by matter*, *Phys. Rev. D* **104** (2021) 083508 [[2104.04836](#)].
- [96] J. Bielefeld and R.R. Caldwell, *Cosmological consequences of classical flavor-space locked gauge field radiation*, *Phys. Rev. D* **91** (2015) 124004 [[1503.05222](#)].
- [97] A.D. Miravet and A.L. Maroto, *Imprint of ultralight vector fields on gravitational wave propagation*, *Phys. Rev. D* **103** (2021) 123546 [[2012.07505](#)].
- [98] A.J. Tishue and R.R. Caldwell, *Relic cosmological vector fields and inflationary gravitational waves*, *Phys. Rev. D* **104** (2021) 063531 [[2105.08073](#)].
- [99] A.D. Miravet and A.L. Maroto, *Vector dark radiation and gravitational-wave polarization*, [2203.07125](#).
- [100] K. Ichiki, M. Yamaguchi and J. Yokoyama, *Lepton asymmetry in the primordial gravitational wave spectrum*, *Phys. Rev. D* **75** (2007) 084017 [[hep-ph/0611121](#)].
- [101] M. Valle, *Kinetic theory and evolution of cosmological fluctuations with neutrino number asymmetry*, *Phys. Rev. D* **88** (2013) 041304 [[1307.0392](#)].
- [102] A. Sadofyev and S. Sen, *Chiral Anomalous Dispersion*, *JHEP* **02** (2018) 099 [[1712.03956](#)].
- [103] P. Gubler, N. Yamamoto and D.-L. Yang, *Chiral gravitational waves from thermalized neutrinos in the early Universe*, [2205.10516](#).
- [104] L.R.W. Abramo, R.H. Brandenberger and V.F. Mukhanov, *The Energy - momentum tensor for cosmological perturbations*, *Phys. Rev. D* **56** (1997) 3248 [[gr-qc/9704037](#)].
- [105] R. Brandenberger and T. Takahashi, *Back-Reaction of Gravitational Waves Revisited*, *JCAP* **07** (2018) 040 [[1805.02424](#)].
- [106] T.J. Clarke, E.J. Copeland and A. Moss, *Constraints on primordial gravitational waves from the Cosmic Microwave Background*, *JCAP* **10** (2020) 002 [[2004.11396](#)].
- [107] C.-P. Ma and E. Bertschinger, *Cosmological perturbation theory in the synchronous and conformal Newtonian gauges*, *Astrophys. J.* **455** (1995) 7 [[astro-ph/9506072](#)].
- [108] S. Weinberg, *Cosmology*, Oxford University Press (2008).
- [109] K.N. Abazajian et al., *Synergy between cosmological and laboratory searches in neutrino physics: a white paper*, [2203.07377](#).

- [110] J.M. Berryman et al., *Neutrino Self-Interactions: A White Paper*, in *2022 Snowmass Summer Study*, 3, 2022 [[2203.01955](#)].
- [111] G. Raffelt and J. Silk, *LIGHT NEUTRINOS AS COLD DARK MATTER*, *Phys. Lett. B* **192** (1987) 65.
- [112] A.V. Berkov, Y.P. Nikitin, A.L. Sudarikov and M.Y. Khlopov, *POSSIBLE EXPERIMENTAL SEARCH FOR ANOMALOUS $\bar{\nu}\nu$ NEUTRINO INTERACTION. (IN RUSSIAN)*, *Yad. Fiz.* **46** (1987) 1729.
- [113] A.V. Berkov, Y.P. Nikitin, A.L. Sudarikov and M.Y. Khlopov, *POSSIBLE MANIFESTATIONS OF ANOMALOUS $\bar{\nu}\nu$ NEUTRINO INTERACTION. (IN RUSSIAN)*, *Sov. J. Nucl. Phys.* **48** (1988) 497.
- [114] K.M. Belotsky, A.L. Sudarikov and M.Y. Khlopov, *Constraint on anomalous $\bar{\nu}\nu$ interaction*, *Phys. Atom. Nucl.* **64** (2001) 1637.
- [115] Z. Chacko, L.J. Hall, T. Okui and S.J. Oliver, *CMB signals of neutrino mass generation*, *Phys. Rev. D* **70** (2004) 085008 [[hep-ph/0312267](#)].
- [116] S. Hannestad, *Structure formation with strongly interacting neutrinos - Implications for the cosmological neutrino mass bound*, *JCAP* **02** (2005) 011 [[astro-ph/0411475](#)].
- [117] S. Hannestad and G. Raffelt, *Constraining invisible neutrino decays with the cosmic microwave background*, *Phys. Rev. D* **72** (2005) 103514 [[hep-ph/0509278](#)].
- [118] N.F. Bell, E. Pierpaoli and K. Sigurdson, *Cosmological signatures of interacting neutrinos*, *Phys. Rev. D* **73** (2006) 063523 [[astro-ph/0511410](#)].
- [119] M. Cirelli and A. Strumia, *Cosmology of neutrinos and extra light particles after WMAP3*, *JCAP* **12** (2006) 013 [[astro-ph/0607086](#)].
- [120] A. Friedland, K.M. Zurek and S. Bashinsky, *Constraining Models of Neutrino Mass and Neutrino Interactions with the Planck Satellite*, [0704.3271](#).
- [121] A. Basboll, O.E. Bjaelde, S. Hannestad and G.G. Raffelt, *Are cosmological neutrinos free-streaming?*, *Phys. Rev. D* **79** (2009) 043512 [[0806.1735](#)].
- [122] Z. Bialynicka-Birula, *Do Neutrinos Interact between Themselves?*, *Nuovo Cim.* **33** (1964) 1484.
- [123] M. Archidiacono and S. Hannestad, *Updated constraints on non-standard neutrino interactions from Planck*, *JCAP* **07** (2014) 046 [[1311.3873](#)].
- [124] M. Archidiacono, S. Hannestad, R.S. Hansen and T. Tram, *Cosmology with self-interacting sterile neutrinos and dark matter - A pseudoscalar model*, *Phys. Rev. D* **91** (2015) 065021 [[1404.5915](#)].
- [125] F. Forastieri, M. Lattanzi and P. Natoli, *Constraints on secret neutrino interactions after Planck*, *JCAP* **07** (2015) 014 [[1504.04999](#)].
- [126] X. Chu, B. Dasgupta and J. Kopp, *Sterile neutrinos with secret interactions—lasting friendship with cosmology*, *JCAP* **10** (2015) 011 [[1505.02795](#)].
- [127] Y. Farzan and S. Hannestad, *Neutrinos secretly converting to lighter particles to please both KATRIN and the cosmos*, *JCAP* **02** (2016) 058 [[1510.02201](#)].
- [128] F. Forastieri, M. Lattanzi, G. Mangano, A. Mirizzi, P. Natoli and N. Saviano, *Cosmic microwave background constraints on secret interactions among sterile neutrinos*, *JCAP* **07** (2017) 038 [[1704.00626](#)].
- [129] S.M. Kocsibang and S. Hannestad, *Constraining dynamical neutrino mass generation with cosmological data*, *JCAP* **09** (2017) 014 [[1707.02579](#)].
- [130] E. Di Valentino, C. Bøehm, E. Hivon and F.R. Bouchet, *Reducing the H_0 and σ_8 tensions with Dark Matter-neutrino interactions*, *Phys. Rev. D* **97** (2018) 043513 [[1710.02559](#)].
- [131] N. Song, M.C. Gonzalez-Garcia and J. Salvado, *Cosmological constraints with self-interacting sterile neutrinos*, *JCAP* **10** (2018) 055 [[1805.08218](#)].
- [132] C.D. Kreisch, F.-Y. Cyr-Racine and O. Doré, *Neutrino puzzle: Anomalies, interactions, and cosmological tensions*, *Phys. Rev. D* **101** (2020) 123505 [[1902.00534](#)].
- [133] F. Forastieri, M. Lattanzi and P. Natoli, *Cosmological constraints on neutrino self-interactions with a light mediator*, *Phys. Rev. D* **100** (2019) 103526 [[1904.07810](#)].

- [134] S. Roy Choudhury, S. Hannestad and T. Tram, *Updated constraints on massive neutrino self-interactions from cosmology in light of the H_0 tension*, *JCAP* **03** (2021) 084 [[2012.07519](#)].
- [135] I. Esteban and J. Salvado, *Long Range Interactions in Cosmology: Implications for Neutrinos*, *JCAP* **05** (2021) 036 [[2101.05804](#)].
- [136] Y. Du and J.-H. Yu, *Neutrino non-standard interactions meet precision measurements of N_{eff}* , *JHEP* **05** (2021) 058 [[2101.10475](#)].
- [137] J. Venzor, G. Garcia-Arroyo, A. Pérez-Lorenzana and J. De-Santiago, *Massive neutrino self-interactions with a light mediator in cosmology*, [2202.09310](#).
- [138] G. Mangano, A. Melchiorri, P. Serra, A. Cooray and M. Kamionkowski, *Cosmological bounds on dark matter-neutrino interactions*, *Phys. Rev. D* **74** (2006) 043517 [[astro-ph/0606190](#)].
- [139] P. Serra, F. Zalamea, A. Cooray, G. Mangano and A. Melchiorri, *Constraints on neutrino – dark matter interactions from cosmic microwave background and large scale structure data*, *Phys. Rev. D* **81** (2010) 043507 [[0911.4411](#)].
- [140] J.A.D. Diacounis and Y.Y.Y. Wong, *Using CMB spectral distortions to distinguish between dark matter solutions to the small-scale crisis*, *JCAP* **09** (2017) 011 [[1707.07050](#)].
- [141] S. Ghosh, R. Khatri and T.S. Roy, *Dark neutrino interactions make gravitational waves blue*, *Phys. Rev. D* **97** (2018) 063529 [[1711.09929](#)].
- [142] M.R. Mosbech, C. Boehm, S. Hannestad, O. Mena, J. Stadler and Y.Y.Y. Wong, *The full Boltzmann hierarchy for dark matter-massive neutrino interactions*, *JCAP* **03** (2021) 066 [[2011.04206](#)].
- [143] A. Paul, A. Chatterjee, A. Ghoshal and S. Pal, *Shedding light on dark matter and neutrino interactions from cosmology*, *JCAP* **10** (2021) 017 [[2104.04760](#)].
- [144] D. Green, D.E. Kaplan and S. Rajendran, *Neutrino interactions in the late universe*, *JHEP* **11** (2021) 162 [[2108.06928](#)].
- [145] F.-Y. Cyr-Racine and K. Sigurdson, *Cosmology of atomic dark matter*, *Phys. Rev. D* **87** (2013) 103515 [[1209.5752](#)].
- [146] K.S. Jeong and F. Takahashi, *Self-interacting Dark Radiation*, *Phys. Lett. B* **725** (2013) 134 [[1305.6521](#)].
- [147] F.-Y. Cyr-Racine, R. de Putter, A. Raccanelli and K. Sigurdson, *Constraints on Large-Scale Dark Acoustic Oscillations from Cosmology*, *Phys. Rev. D* **89** (2014) 063517 [[1310.3278](#)].
- [148] M.A. Buen-Abad, G. Marques-Tavares and M. Schmaltz, *Non-Abelian dark matter and dark radiation*, *Phys. Rev. D* **92** (2015) 023531 [[1505.03542](#)].
- [149] Z. Chacko, Y. Cui, S. Hong and T. Okui, *Hidden dark matter sector, dark radiation, and the CMB*, *Phys. Rev. D* **92** (2015) 055033 [[1505.04192](#)].
- [150] J. Lesgourgues, G. Marques-Tavares and M. Schmaltz, *Evidence for dark matter interactions in cosmological precision data?*, *JCAP* **02** (2016) 037 [[1507.04351](#)].
- [151] Y. Tang, *Interacting Scalar Radiation and Dark Matter in Cosmology*, *Phys. Lett. B* **757** (2016) 387 [[1603.00165](#)].
- [152] P. Ko and Y. Tang, *Light dark photon and fermionic dark radiation for the Hubble constant and the structure formation*, *Phys. Lett. B* **762** (2016) 462 [[1608.01083](#)].
- [153] Z. Chacko, Y. Cui, S. Hong, T. Okui and Y. Tsai, *Partially Acoustic Dark Matter, Interacting Dark Radiation, and Large Scale Structure*, *JHEP* **12** (2016) 108 [[1609.03569](#)].
- [154] V. Prilepina and Y. Tsai, *Reconciling Large And Small-Scale Structure In Twin Higgs Models*, *JHEP* **09** (2017) 033 [[1611.05879](#)].
- [155] C. Brust, Y. Cui and K. Sigurdson, *Cosmological Constraints on Interacting Light Particles*, *JCAP* **08** (2017) 020 [[1703.10732](#)].
- [156] R. Krall, F.-Y. Cyr-Racine and C. Dvorkin, *Wandering in the Lyman-alpha Forest: A Study of Dark Matter-Dark Radiation Interactions*, *JCAP* **09** (2017) 003 [[1705.08894](#)].

- [157] M.A. Buen-Abad, M. Schmaltz, J. Lesgourgues and T. Brinckmann, *Interacting Dark Sector and Precision Cosmology*, *JCAP* **01** (2018) 008 [[1708.09406](#)].
- [158] Z. Pan, M. Kaplinghat and L. Knox, *Searching for Signatures of Dark matter-Dark Radiation Interaction in Observations of Large-scale Structure*, *Phys. Rev. D* **97** (2018) 103531 [[1801.07348](#)].
- [159] Z. Chacko, D. Curtin, M. Geller and Y. Tsai, *Cosmological Signatures of a Mirror Twin Higgs*, *JHEP* **09** (2018) 163 [[1803.03263](#)].
- [160] M. Garny, T. Konstandin, L. Sagunski and S. Tulin, *Lyman- α forest constraints on interacting dark sectors*, *JCAP* **09** (2018) 011 [[1805.12203](#)].
- [161] M. Archidiacono, D.C. Hooper, R. Murgia, S. Bohr, J. Lesgourgues and M. Viel, *Constraining Dark Matter-Dark Radiation interactions with CMB, BAO, and Lyman- α* , *JCAP* **10** (2019) 055 [[1907.01496](#)].
- [162] S. Bansal, J.H. Kim, C. Kolda, M. Low and Y. Tsai, *Mirror twin Higgs cosmology: constraints and a possible resolution to the H_0 and S_8 tensions*, *JHEP* **05** (2022) 050 [[2110.04317](#)].
- [163] M.A. Corona, R. Murgia, M. Cadeddu, M. Archidiacono, S. Gariazzo, C. Giunti et al., *Pseudoscalar sterile neutrino self-interactions in light of Planck, SPT and ACT data*, [2112.00037](#).
- [164] E. Di Valentino, O. Mena, S. Pan, L. Visinelli, W. Yang, A. Melchiorri et al., *In the realm of the Hubble tension—a review of solutions*, *Class. Quant. Grav.* **38** (2021) 153001 [[2103.01183](#)].
- [165] S. Kumar and R.C. Nunes, *Echo of interactions in the dark sector*, *Phys. Rev. D* **96** (2017) 103511 [[1702.02143](#)].
- [166] N. Blinov, K.J. Kelly, G.Z. Krnjaic and S.D. McDermott, *Constraining the Self-Interacting Neutrino Interpretation of the Hubble Tension*, *Phys. Rev. Lett.* **123** (2019) 191102 [[1905.02727](#)].
- [167] S. Ghosh, R. Khatri and T.S. Roy, *Can dark neutrino interactions phase out the Hubble tension?*, *Phys. Rev. D* **102** (2020) 123544 [[1908.09843](#)].
- [168] M. Escudero and S.J. Witte, *A CMB search for the neutrino mass mechanism and its relation to the Hubble tension*, *Eur. Phys. J. C* **80** (2020) 294 [[1909.04044](#)].
- [169] H.-J. He, Y.-Z. Ma and J. Zheng, *Resolving Hubble Tension by Self-Interacting Neutrinos with Dirac Seesaw*, *JCAP* **11** (2020) 003 [[2003.12057](#)].
- [170] M. Berbig, S. Jana and A. Trautner, *The Hubble tension and a renormalizable model of gauged neutrino self-interactions*, *Phys. Rev. D* **102** (2020) 115008 [[2004.13039](#)].
- [171] N. Becker, D.C. Hooper, F. Kahlhoefer, J. Lesgourgues and N. Schöneberg, *Cosmological constraints on multi-interacting dark matter*, *JCAP* **02** (2021) 019 [[2010.04074](#)].
- [172] G. Choi, T.T. Yanagida and N. Yokozaki, *A model of interacting dark matter and dark radiation for H_0 and σ_8 tensions*, *JHEP* **01** (2021) 127 [[2010.06892](#)].
- [173] A. Mazumdar, S. Mohanty and P. Parashari, *Flavour specific neutrino self-interaction: H_0 tension and IceCube*, [2011.13685](#).
- [174] D. Aloni, A. Berlin, M. Joseph, M. Schmaltz and N. Weiner, *A Step in Understanding the Hubble Tension*, [2111.00014](#).
- [175] M. Joseph, D. Aloni, M. Schmaltz, E.N. Sivarajan and N. Weiner, *A Step in Understanding the S_8 Tension*, [2207.03500](#).
- [176] M.A. Buen-Abad, Z. Chacko, C. Kilic, G. Marques-Tavares and T. Youn, *Stepped Partially Acoustic Dark Matter, Large Scale Structure, and the Hubble Tension*, [2208.05984](#).
- [177] J.M. Stewart, *Perturbations in an Expanding Universe of Free Particles*, *Astrophys. J.* **176** (1972) 323.
- [178] D.A. Dicus and W.W. Repko, *Comment on damping of tensor modes in cosmology*, *Phys. Rev. D* **72** (2005) 088302 [[astro-ph/0509096](#)].
- [179] G. Shchedrin, *Infrared divergence of the gravitational wave damping in the early Universe*, [1204.1384](#).
- [180] B.A. Stefanek and W.W. Repko, *Analytic description of the damping of gravitational waves by free streaming neutrinos*, *Phys. Rev. D* **88** (2013) 083536 [[1207.7285](#)].

- [181] A. Rebhan, *Analytical solutions for cosmological perturbations with relativistic collisionless matter*, *Nucl. Phys. B* **368** (1992) 479.
- [182] H. Nachbagauer, A.K. Rebhan and D.J. Schwarz, *The Dynamics of cosmological perturbations in thermal $\lambda\phi^4$ theory*, *Phys. Rev. D* **53** (1996) 5468 [[gr-qc/9510046](#)].
- [183] M. Kamionkowski, *Cosmological perturbations without the Boltzmann hierarchy*, *Phys. Rev. D* **104** (2021) 063512 [[2105.02887](#)].
- [184] L. Ji, M. Kamionkowski and J.L. Bernal, *Cosmological perturbations: non-cold relics without the Boltzmann hierarchy*, [2201.11129](#).
- [185] S. Bashinsky, *Coupled evolution of primordial gravity waves and relic neutrinos*, [astro-ph/0505502](#).
- [186] Y. Watanabe and E. Komatsu, *Improved Calculation of the Primordial Gravitational Wave Spectrum in the Standard Model*, *Phys. Rev. D* **73** (2006) 123515 [[astro-ph/0604176](#)].
- [187] C. Caprini, R. Durrer, T. Konstandin and G. Servant, *General Properties of the Gravitational Wave Spectrum from Phase Transitions*, *Phys. Rev. D* **79** (2009) 083519 [[0901.1661](#)].
- [188] K.N. Ananda, C. Clarkson and D. Wands, *The Cosmological gravitational wave background from primordial density perturbations*, *Phys. Rev. D* **75** (2007) 123518 [[gr-qc/0612013](#)].
- [189] D. Baumann, P.J. Steinhardt, K. Takahashi and K. Ichiki, *Gravitational Wave Spectrum Induced by Primordial Scalar Perturbations*, *Phys. Rev. D* **76** (2007) 084019 [[hep-th/0703290](#)].
- [190] G. Domènech, *Scalar Induced Gravitational Waves Review*, *Universe* **7** (2021) 398 [[2109.01398](#)].
- [191] S. Saga, K. Ichiki and N. Sugiyama, *Impact of anisotropic stress of free-streaming particles on gravitational waves induced by cosmological density perturbations*, *Phys. Rev. D* **91** (2015) 024030 [[1412.1081](#)].
- [192] D. Blas, J. Lesgourgues and T. Tram, *The Cosmic Linear Anisotropy Solving System (CLASS) II: Approximation schemes*, *JCAP* **07** (2011) 034 [[1104.2933](#)].
- [193] J.C. Hill et al., *Atacama Cosmology Telescope: Constraints on prerecombination early dark energy*, *Phys. Rev. D* **105** (2022) 123536 [[2109.04451](#)].
- [194] V. Poulin, T.L. Smith and A. Bartlett, *Dark energy at early times and ACT data: A larger Hubble constant without late-time priors*, *Phys. Rev. D* **104** (2021) 123550 [[2109.06229](#)].
- [195] A. La Posta, T. Louis, X. Garrido and J.C. Hill, *Constraints on prerecombination early dark energy from SPT-3G public data*, *Phys. Rev. D* **105** (2022) 083519 [[2112.10754](#)].
- [196] T.L. Smith, M. Lucca, V. Poulin, G.F. Abellan, L. Balkenhol, K. Benabed et al., *Hints of Early Dark Energy in Planck, SPT, and ACT data: new physics or systematics?*, [2202.09379](#).
- [197] X.-J. Liu, W. Zhao, Y. Zhang and Z.-H. Zhu, *Detecting Relic Gravitational Waves by Pulsar Timing Arrays: Effects of Cosmic Phase Transitions and Relativistic Free-Streaming Gases*, *Phys. Rev. D* **93** (2016) 024031 [[1509.03524](#)].
- [198] BICEP2, KECK ARRAY collaboration, *BICEP2 / Keck Array x: Constraints on Primordial Gravitational Waves using Planck, WMAP, and New BICEP2/Keck Observations through the 2015 Season*, *Phys. Rev. Lett.* **121** (2018) 221301 [[1810.05216](#)].
- [199] K. Schmitz, *New Sensitivity Curves for Gravitational-Wave Signals from Cosmological Phase Transitions*, *JHEP* **01** (2021) 097 [[2002.04615](#)].
- [200] K. Schmitz, *New Sensitivity Curves for Gravitational-Wave Experiments*, Feb., 2020. [10.5281/zenodo.3689582](#).
- [201] A. Sesana et al., *Unveiling the gravitational universe at μ -Hz frequencies*, *Exper. Astron.* **51** (2021) 1333 [[1908.11391](#)].
- [202] C. Dvorkin et al., *The Physics of Light Relics*, in *2022 Snowmass Summer Study*, 3, 2022 [[2203.07943](#)].
- [203] F. Niedermann and M.S. Sloth, *Resolving the Hubble tension with new early dark energy*, *Phys. Rev. D* **102** (2020) 063527 [[2006.06686](#)].
- [204] F. Niedermann and M.S. Sloth, *Hot new early dark energy*, *Phys. Rev. D* **105** (2022) 063509 [[2112.00770](#)].

- [205] D. Cyncynates, O. Simon, J.O. Thompson and Z.J. Weiner, *Nonperturbative structure in coupled axion sectors and implications for direct detection*, [2208.05501](#).
- [206] C.R. Harris et al., *Array programming with NumPy*, *Nature* **585** (2020) 357 [[2006.10256](#)].
- [207] P. Virtanen et al., *SciPy 1.0—Fundamental Algorithms for Scientific Computing in Python*, *Nature Meth.* **17** (2020) 261 [[1907.10121](#)].
- [208] J.D. Hunter, *Matplotlib: A 2D Graphics Environment*, *Comput. Sci. Eng.* **9** (2007) 90.
- [209] A. Meurer et al., *SymPy: symbolic computing in Python*, *PeerJ Comput. Sci.* **3** (2017) e103.
- [210] F. Johansson et al., *mpmath: a Python library for arbitrary-precision floating-point arithmetic (version 0.18)*, December, 2013.
- [211] E. van der Velden, *CMasher: Scientific colormaps for making accessible, informative and 'cmashing' plots*, *The Journal of Open Source Software* **5** (2020) 2004 [[2003.01069](#)].
- [212] E. Hairer, S.P. Nørsett and G. Wanner, *Solving Ordinary Differential Equations I (2nd Revised. Ed.): Nonstiff Problems*, Springer-Verlag, Berlin, Heidelberg (1993).
- [213] E. Hairer, S. Nørsett and G. Wanner, *Solving Ordinary Differential Equations II: Stiff and Differential-Algebraic Problems*, Solving Ordinary Differential Equations II: Stiff and Differential-algebraic Problems, Springer (1993).
- [214] J.R. Pritchard and M. Kamionkowski, *Cosmic microwave background fluctuations from gravitational waves: An Analytic approach*, *Annals Phys.* **318** (2005) 2 [[astro-ph/0412581](#)].